Fast Radio Bursts

Steven Saliterman

1. Observation of Fast Radio Bursts (FRBs).
   - Dispersion measure (DM).
   - First FRB identified by Lorimer et al. 2007.
   - The first galactic FRB detected 2020.
   - Localization
2. Emissions
   - Review of astrophysical radiation mechanisms.
   - Why is coherent emission observed?
   - Difference between coherent & non-coherent.
3. Progenitors
   - Source models
   - Beaming.
   - Repeaters & sub-burst frequency drift.

CHIME
Kaleden, BC

Parks
Australia

Jansky VLA
NM

LOFAR
Netherlands

NASA/JPL-Caltech Magnetar Depiction

(1) CHIME; (2) Shatelle Shaw; (3) Bettymaya Foott, (4) LOFAR

Fast Radio Bursts (FRB)

- *Microsecond-millisecond* radio wave bursts of high luminosity.
- *Occurrences*, all-sky FRB rate is 1000-10,000 per day.
- Non-repeating and repeating varieties. (May be that all repeat!)
- *Frequency range* of ~400 MHz to 8 GHz.
- *Isotropic energies* follow a power-law distribution with a possible exponential cut-off.[3] $\sim 10^{38}$–10^{46} erg s^{-1}
- *Located* largely outside the Milky Way based on large dispersive delays. These are frequency dependent time delays from cold ionized plasma of free electrons along the pathway. There is a DM-FRB redshift relationship (DM_{cosmic} vs z_{FRB}).
- Possible *progenitors* include(1) isolated or binary compact objects (white dwarfs, neutron stars - e.g. magnetars, and black holes); or (2) Active Galactic Nuclei (AGN).

Cordes JM, Chatterjee S. Fast Radio Bursts: An Extragalactic Enigma. *ARA & A*. 2019;57(1):417-465. doi:10.1146/annurev-astro-091918-104501.
Petroff E, Hessels JWT, Lorimer DR. Fast radio bursts. *The Astronomy and Astrophysics Review*. 2019/05/24 2019;27(1):4. doi:10.1007/s00159-019-0116-6. P4.
Zhang RC, Zhang B, Li Y, Lorimer DR. On the energy and redshift distributions of fast radio bursts. Monthly Notices of the Royal Astronomical Society. 2021;501(1):157-167. doi:10.1093/mnras/staa3537

Timeline

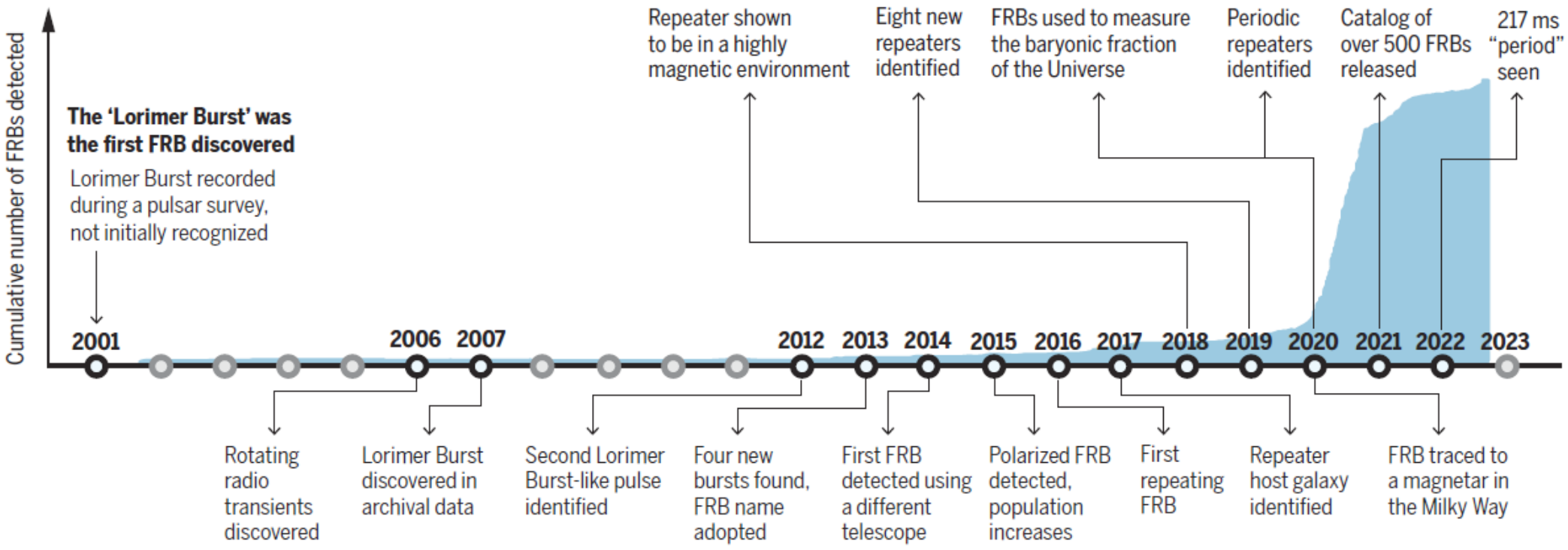

Timeline of some important breakthroughs in FRBs. The blue graph indicates the cumulative number of FRBs detected (~800, including some bursts from repeaters). Source: HeRTA: FRBSTATS online catalog.

- Compact objects like NS *rapidly rotating magnetars* are attractive because of the burst rates, repeatability and energetics. They are of sufficient number, and posses sufficient free energy – rotation, magnetic and gravitational.
- *Energy densities* 10^{10} - 10^{14} greater than galactic pulsars.
- *Interferometric* followup of a FRB allows sub-arcsecond localization.
- Useful *tracers* of circumsource environments.
- *Coherent* since the emission is too bright to be explained by electrons emitted separately. *Grouping of multiple coherent events giving a multipeaked incoherent signal*. (Contrast this to years-long incoherent thermal radio emissions from a SN explosion.)

Cordes JM, Chatterjee S. Fast Radio Bursts: An Extragalactic Enigma. *ARA & A*. 2019;57(1):417-465. doi:10.1146/annurev-astro-091918-104501

Illustration of the Path of an FRB to the MW

- FRB detected by the Australian Square KM Array Pathfinder (ASKP) June 10, 2022.
- This is 8 billion years old, with release of the Sun's total emissions over 30 years in just ms.
- Source galaxy determined by the European Southern Observatory (ESO) Very Large Telescope (VLT) in Chile.
- FRB pulses are dispersed by plasma during propagation – the line-of-sight free electron density (n_e).
- This effect is quantified by the FRB Dispersion Measure (DM_{FRB}).

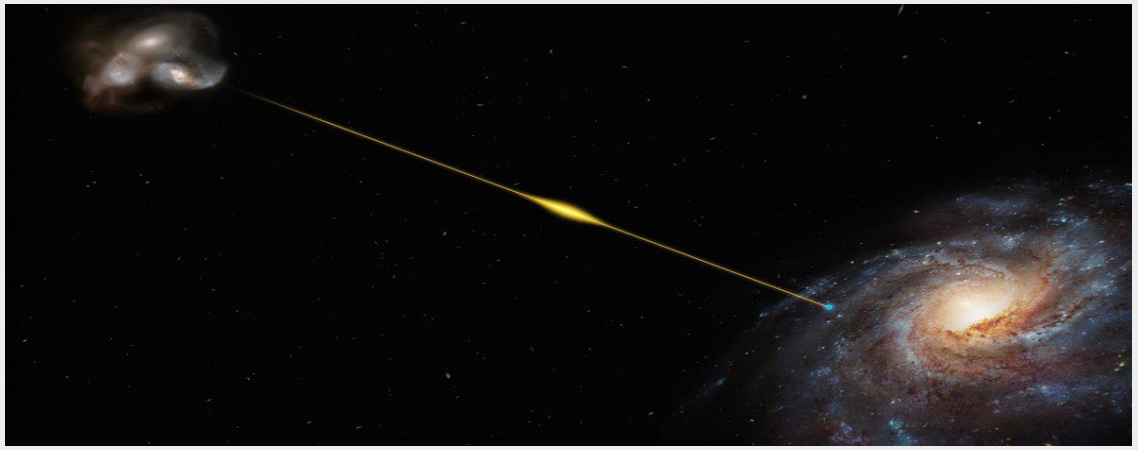

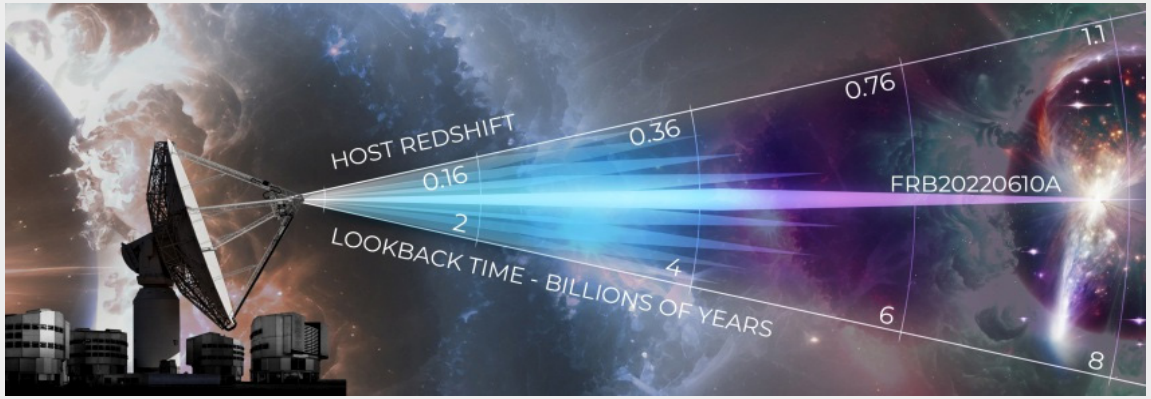

Top: Fast radio burst FRB 20220610A. Credit: ESO/M. Kornmesser.
Bottom: Carl Knox/OzGrav/Swinburne University

Simha S, Lee K-G, Prochaska JX, et al. Searching for the Sources of Excess Extragalactic Dispersion of FRBs. *The Astrophysical journal*. 2023;954(1):71. doi:10.3847/1538-4357/ace324

Cold-Plasma Dispersion

- The signal propagating through the ionized plasma experiences a frequency dependent delay across the frequency band due to the dispersive effects of the plasma.

  The difference in the arrival time is then:

$$\Delta t = 4.148808 \text{ ms} \times \left[\left(\frac{f_{\text{low}}}{\text{GHz}} \right)^{-2} - \left(\frac{f_{\text{high}}}{\text{GHz}} \right)^{-2} \right] \times \text{DM}$$

$$\textit{Where} \frac{e^2}{2\pi m_e c} = 4.148808 \text{ ms; and DM is in pc-cm}^{-3}$$

Lorimer DR, Bailes M, McLaughlin MA, Narkevic DJ, Crawford F. Bright Millisecond Radio Burst of Extragalactic Origin. *Science (American Association for the Advancement of Science). Supplemental material*

Dispersion Measure (DM)

- The $\mathrm{DM_{FRB}}$ measurement represents the electron density n_e, weighted by $(1 + z)^{-1}$, integrating over all physical distance increments ds to a given FRB:

$$\mathrm{DM_{FRB}}\,\frac{\mathrm{pc}}{\mathrm{cm}^3} = \int_0^s \frac{n_e}{(1+z)}\,ds$$

$$\mathrm{DM_{FRB}}(z) = \mathrm{DM_{MW\text{-}ISM}} + \mathrm{DM_{MW\ halo}} + \mathrm{DM_{IGM}}(z) + \mathrm{DM_{host}}(z)$$

The $(1 + z)$ factor accounts for cosmological time dilation for a source at redshift z.

Macquart JP, Prochaska JX, McQuinn M, et al. A census of baryons in the Universe from localized fast radio bursts. *Nature*. 2020/05/01 2020;581(7809):391-395. doi:10.1038/s41586-020-2300-2. Page 392.

Contributions to the DM...

Table 1 Various contributions to the total dispersion measure of an FRB from Eq. 15

Variable	Type	DM contribution (cm^{-3} pc)
DM_{Iono}	Earth ionosphere	$\sim 10^{-5}$
DM_{IPM}	Interplanetary medium of Solar System	$\sim 10^{-3}$
DM_{ISM}	Galactic interstellar medium	$\sim 10^{0} - 10^{3}$
DM_{IGM}	Intergalactic medium	$\sim 10^{2} - 10^{3}$
DM_{Host}	Host galaxy interstellar medium	$\sim 10^{0} - 10^{3}$
DM_{Local}	Local FRB environment	$\sim 10^{0} - 10^{3}$

Petroff E, Hessels JWT, Lorimer DR. Fast radio bursts. *The Astronomy and Astrophysics Review*. 2019/05/24 2019;27(1):4. doi:10.1007/s00159-019-0116-6. Page 16.

Average DM_{cosmic} to Redshift z_{FRB}

$$\left\langle \mathrm{DM}_{\mathrm{cosmic}} \right\rangle = \int_0^{Z_{FRB}} \frac{c\bar{n}_e(z)dz}{H_0(1+z)^2\sqrt{\Omega_m(1+z)^3+\Omega_\Lambda}} \qquad \bar{n}_{\mathrm{e}} = f_{\mathrm{d}}\rho_{\mathrm{b}}(z)m_{\mathrm{p}}^{-1}\left(1-\frac{Y_{HE}}{2}\right)$$

Where m_{p} is proton mass; $Y_{\mathrm{HE}} = 0.25$, mass fraction of helium (DI); $f_{\mathrm{d}}(z)$ is the mass fraction of cosmic baryons; $\rho_{\mathrm{b}}(z) = \Omega_{\mathrm{b}}\rho_{\mathrm{c,o}}(1+z)^3$; and Ω_{m} & Ω_Λ are the matter and dark energy densities today in units of $\rho_{\mathrm{c,o}} = 3H_0^2/8\pi G$. Parameterize Hubbles constant H_0 in terms of dimensionless $h_{70} = H_0/\left(70\ \mathrm{km\ s^{-1}\ Mpc^{-1}}\right)$.

Macquart JP, Prochaska JX, McQuinn M, et al. A census of baryons in the Universe from localized fast radio bursts. *Nature*. 2020/05/01 2020;581(7809):391-395. doi:10.1038/s41586-020-2300-2. Page 392.

DM_{cosmic} vs Redshift (z_{FRB}) for localized FRBs

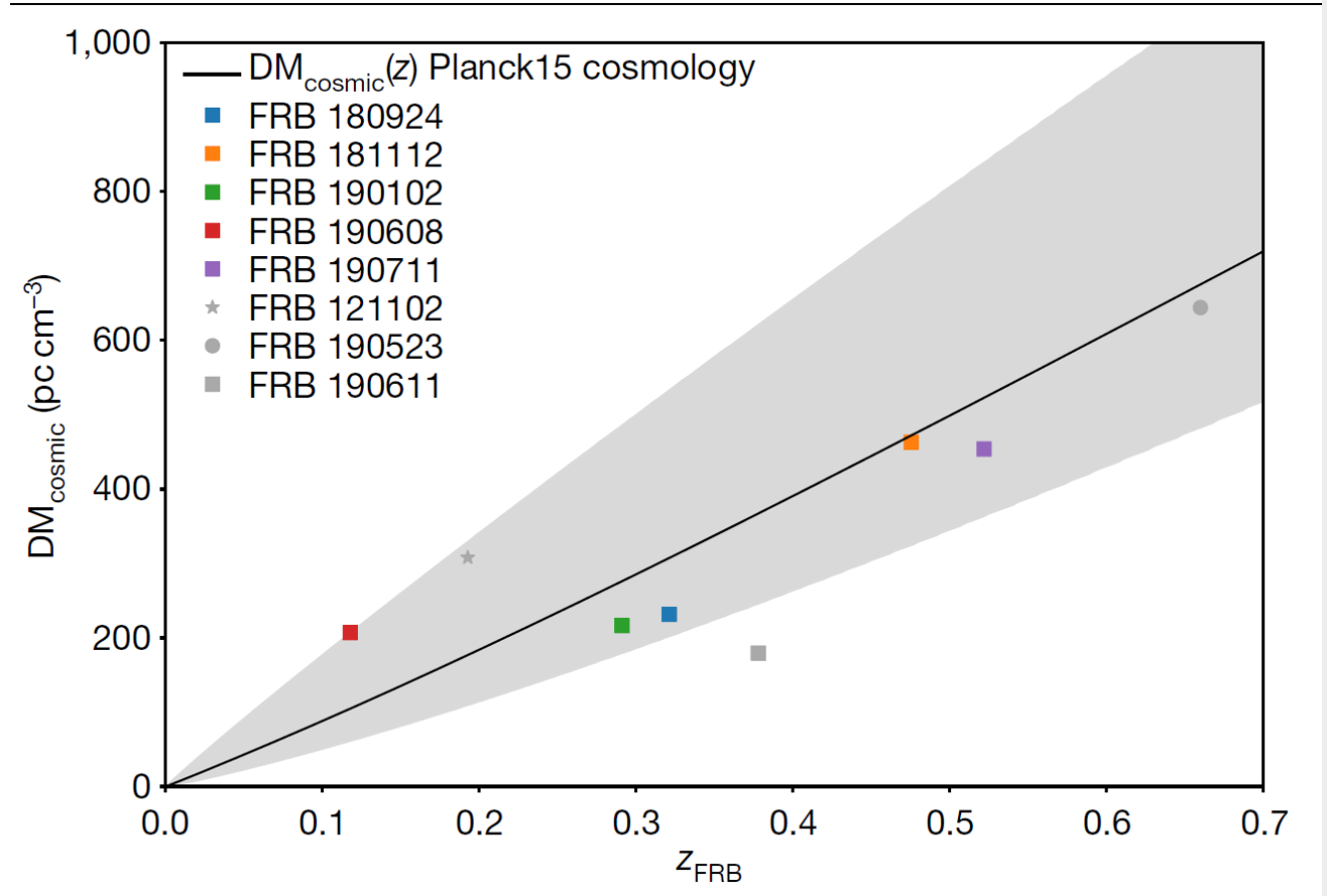

- The DM_{cosmic} values are derived by correcting the observed dispersion measure DM_{FRB} for the estimated contributions from the MW and the FRB host galaxy (the latter assumed here to be $50(1+z)^{-1}$ pc cm^{-3}.
- Scatter is largely consistent with the scatter from the IGM.

Macquart JP, Prochaska JX, McQuinn M, et al. A census of baryons in the Universe from localized fast radio bursts. *Nature*. 2020/05/01 2020;581(7809):391-395. doi:10.1038/s41586-020-2300-2. Page 394.

First FRB Identified by Lorimer et al. 2007

- The burst was discovered in 2007 during a search of *archival data* form a 1.4 GHz survey of the Magellanic Clouds using the multibeam receiver on the 64-m Parkes radio telescope.
- The burst was detected in data taken on *2001 August 24, with DM = 375 cm^{-3} pc* Observed width W = 4.6 ms (f/1.4 GHz)−4.8±0.4, where f is the observing frequency.
- A power-law fit to the mean flux densities obtained in each sub-band yields a spectral index of −4 ± 1.

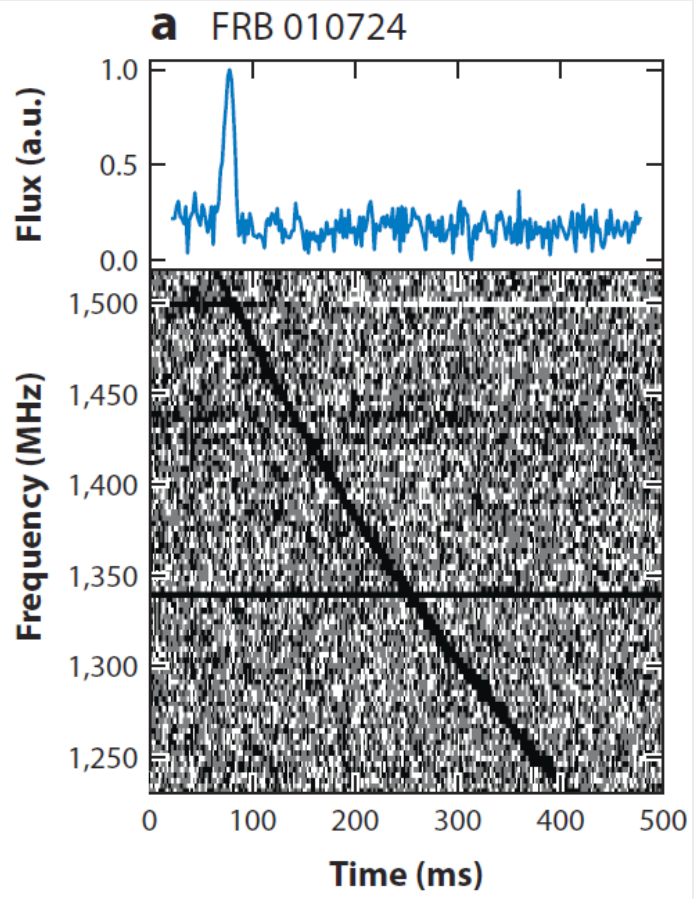

Top: De-dispersed pulse total intensity after frequency averaging across the band (top).
Bottom: Removing the best-fit quadratic pulse dispersion sweep

Lorimer DR, Bailes M, McLaughlin MA, Narkevic DJ, Crawford F. Bright Millisecond Radio Burst of Extragalactic Origin. *Science (American Association for the Advancement of Science)*. 2007;318(5851):777-780. doi:10.1126/science. 1147532

Cordes JM, Chatterjee S. Fast Radio Bursts: An Extragalactic Enigma. *ARA & A*. 2019;57(1):417-465.

First Detected FSB in the Small Magellanic Cloud

- Multi-wavelength image of the field surrounding the burst. The gray scale and contours respectively show Hα and HI emission associated with the SMC.
- Located approximately three degrees south of the center of the Small Magellanic Cloud (SMC).
- Crosses mark the positions of the five known radio pulsars in the SMC and are annotated with their names and DMs in parentheses in units of cm^{-3} pc.
- The open circles show the positions of each of the 13 beams in the survey pointing of diameter equal to the half-power width

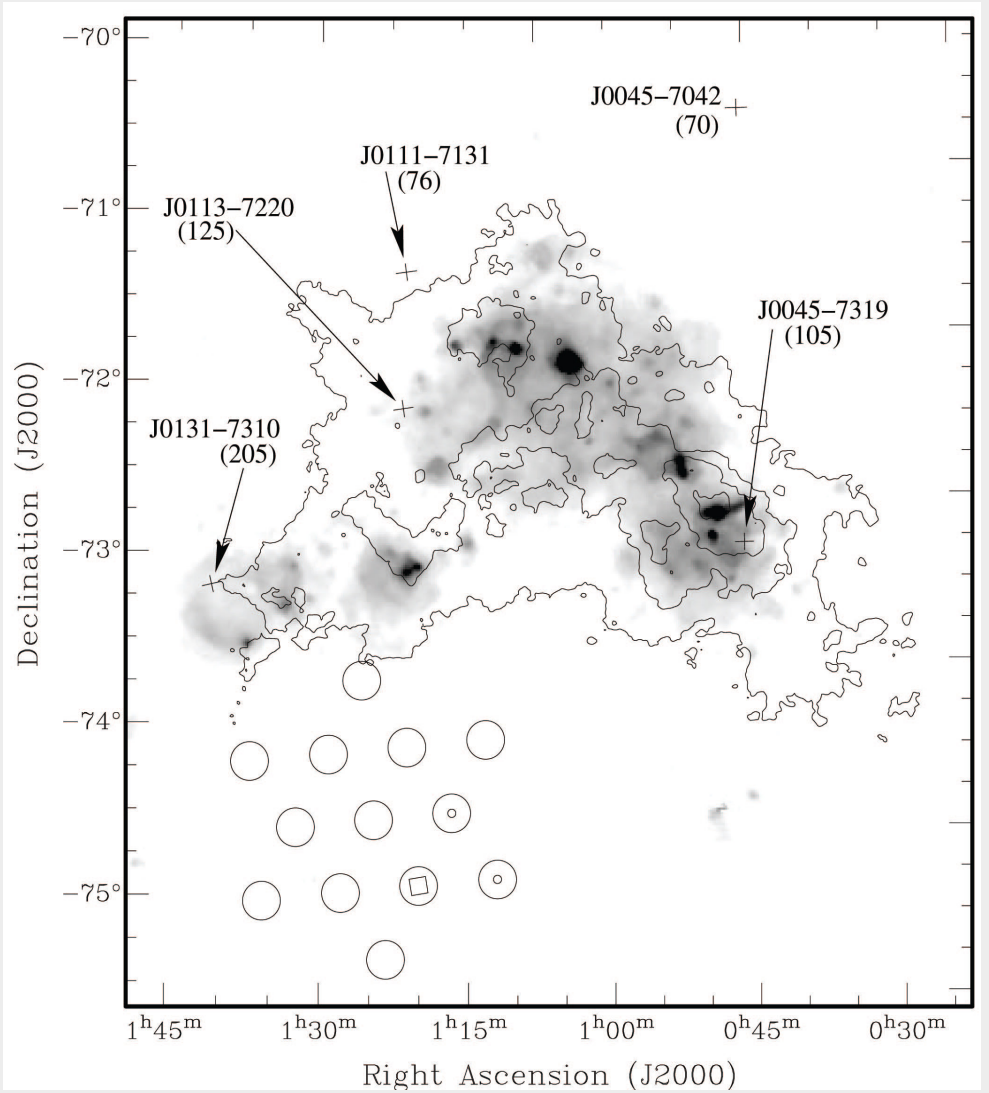

Lorimer DR, Bailes M, McLaughlin MA, Narkevic DJ, Crawford F. Bright Millisecond Radio Burst of Extragalactic Origin. *Science (American Association for the Advancement of Science)*. 2007;318(5851):777-780. doi:10.1126/science.1147532

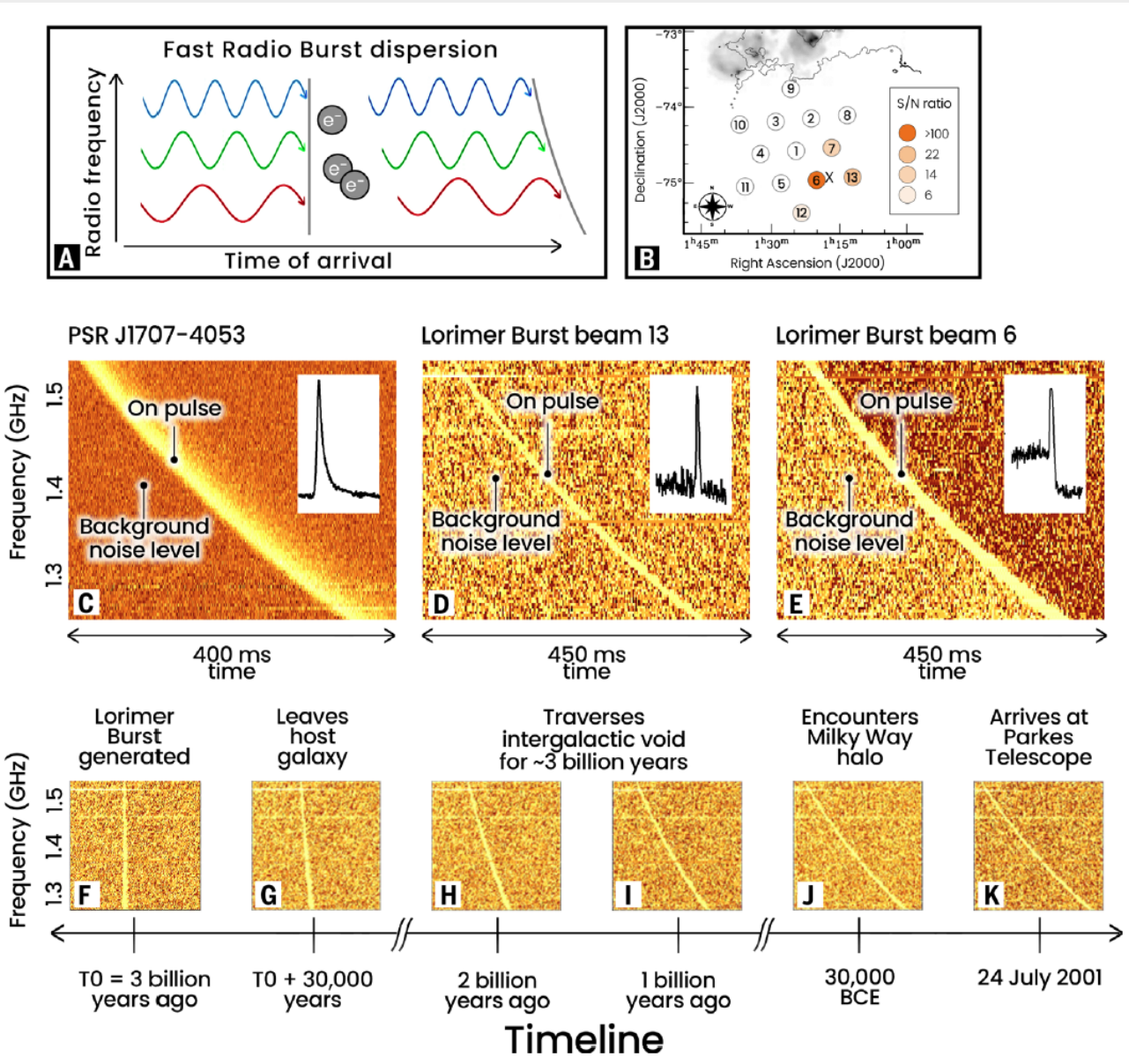

A. Dispersion of the Lorimer Burst. The more energetic (higher-frequency) radio waves (blue) experience less delay than the lower energy waves (red).

B. Pointing of the Parkes 13-Beam receiver just south of the Small Magellanic Cloud.

C. Observed dispersion sweep of the pulsar PSR J1707-4053

D-E. Dispersion sweep of LB, DM=375 pc/cm^{-3} , and integrated pulse profile.

F-K. Inferred evolution over cosmic time.

Bailes M. The discovery and scientific potential of fast radio bursts. *Science*. 2022;378(6620):eabj3043. doi:doi:10.1126/science. abj3043

FRB Dynamic Spectra

Top Panels - the dedispersed pulse total intensity after frequency-averaging across the band

Bottom Panels - the burst on the time–frequency plane after removing the best-fit quadratic pulse dispersion sweep.

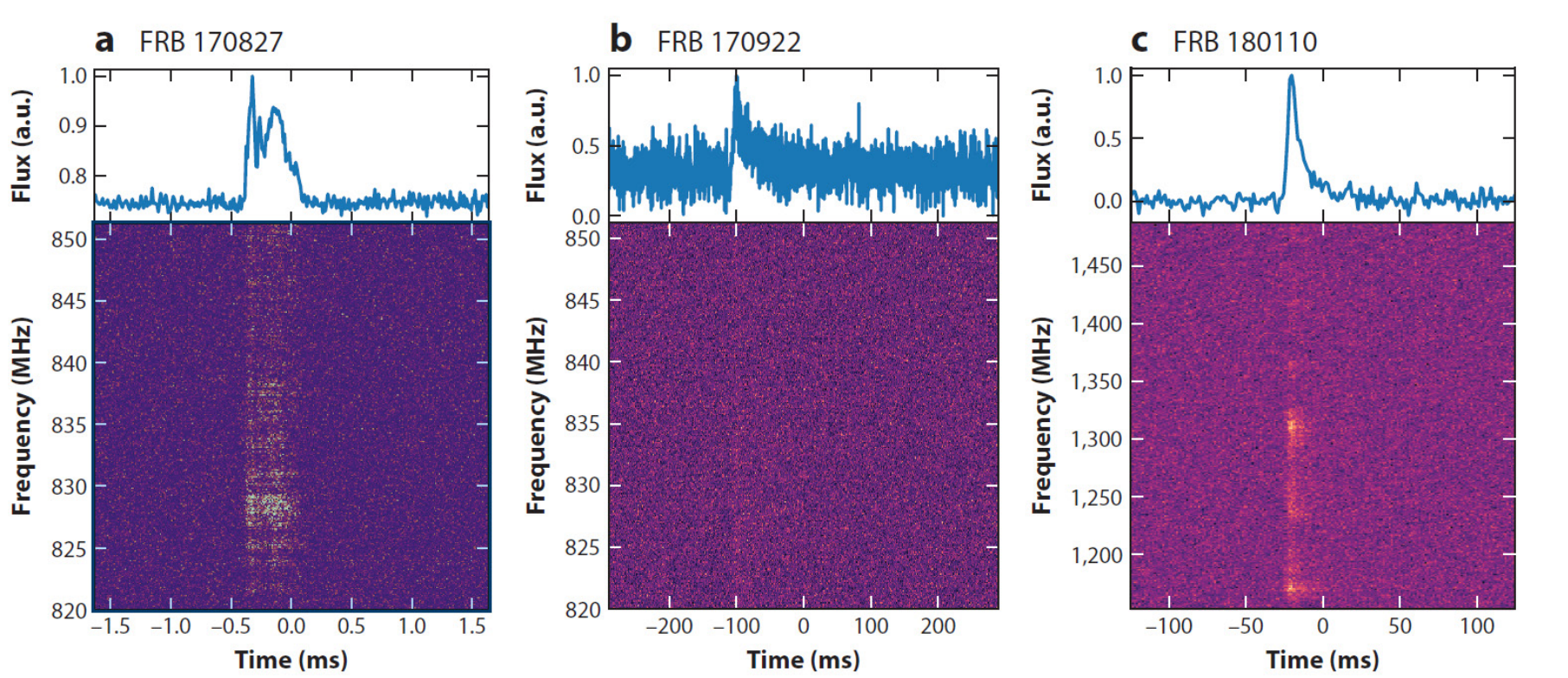

UTMOST | UTMOST | ASKAP

Cordes JM, Chatterjee S. Fast Radio Bursts: An Extragalactic Enigma. *ARA & A*. 2019;57(1):417-465. doi:10.1146/annurev-astro-091918-104501

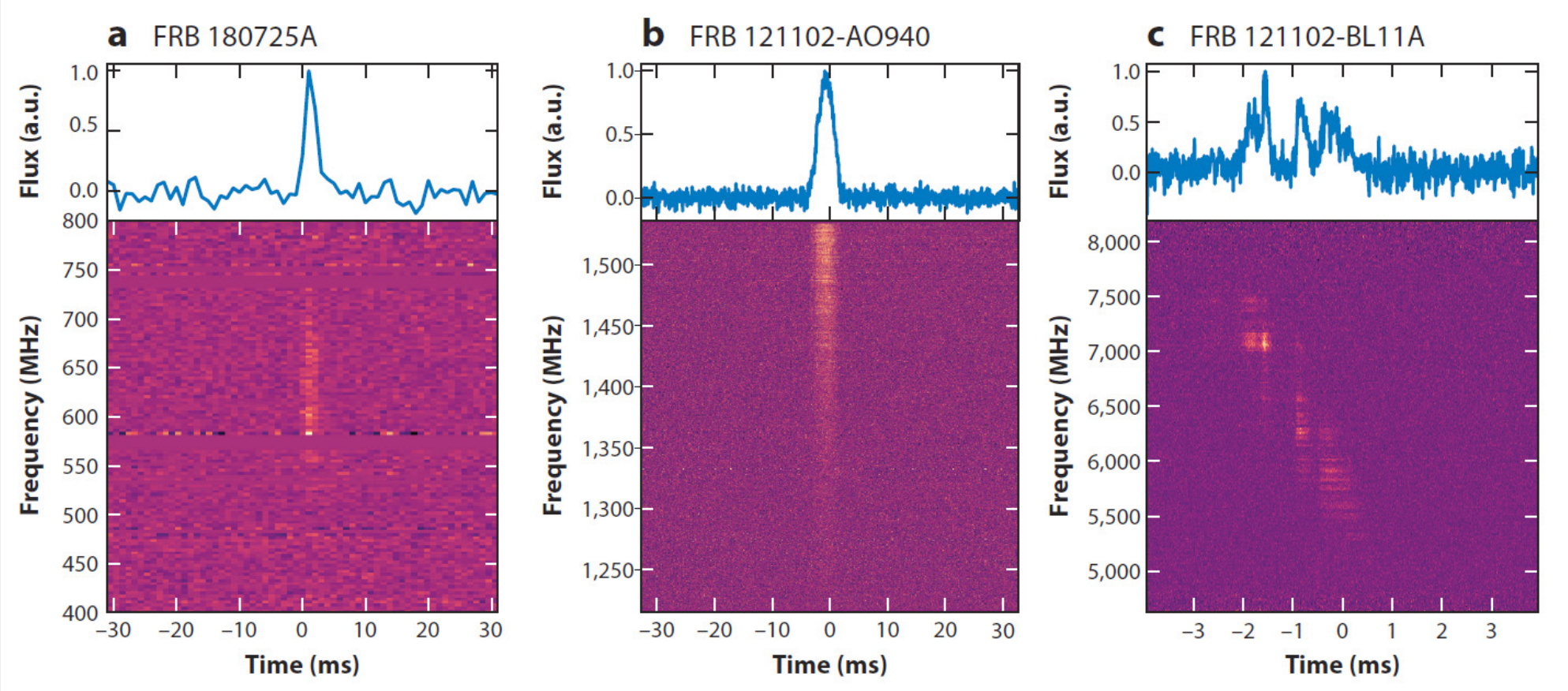

First FRB detected at CHIME down to 550 MHz

First & Brightest at Arecibo at 1.2-1.6 GHz

Greenbank, WV at 4-8 GHz

Cordes JM, Chatterjee S. Fast Radio Bursts: An Extragalactic Enigma. *ARA & A*. 2019;57(1):417-465. doi:10.1146/annurev-astro-091918-104501

Canadian Hydrogen Intensity Mapping Experiment (CHIME)

CHIME & 1 of 3 “Outriggers”

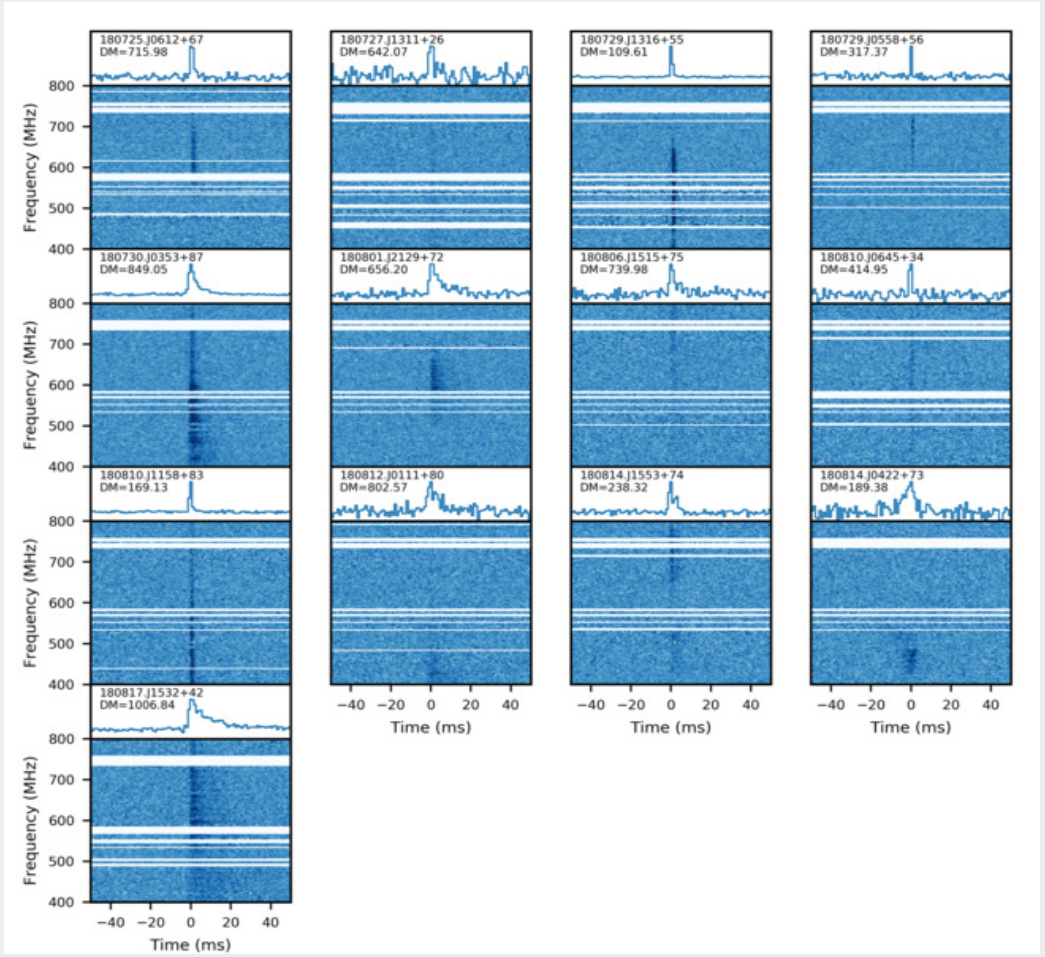

First 13 FRBs found by CHIME/FRB

CHIME

SGR 1935+2154, CHIME

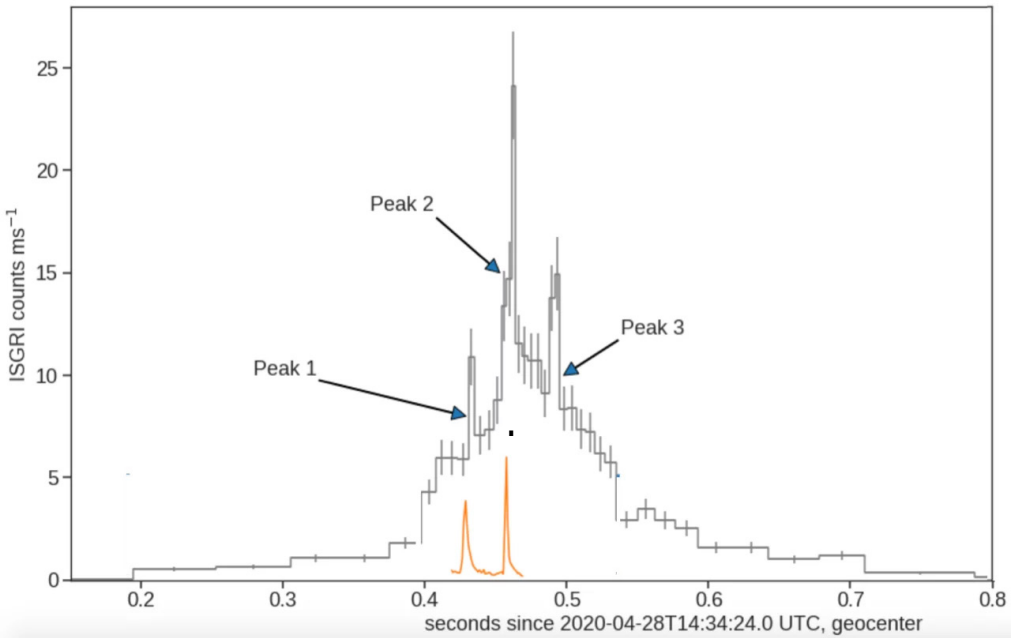

Two FRBs (orange curves) detected by CHIME, during the X-Ray burst (black) observed by INTEGRAL, from the galactic magnetar SGR 1935+2154 4/28/2020.

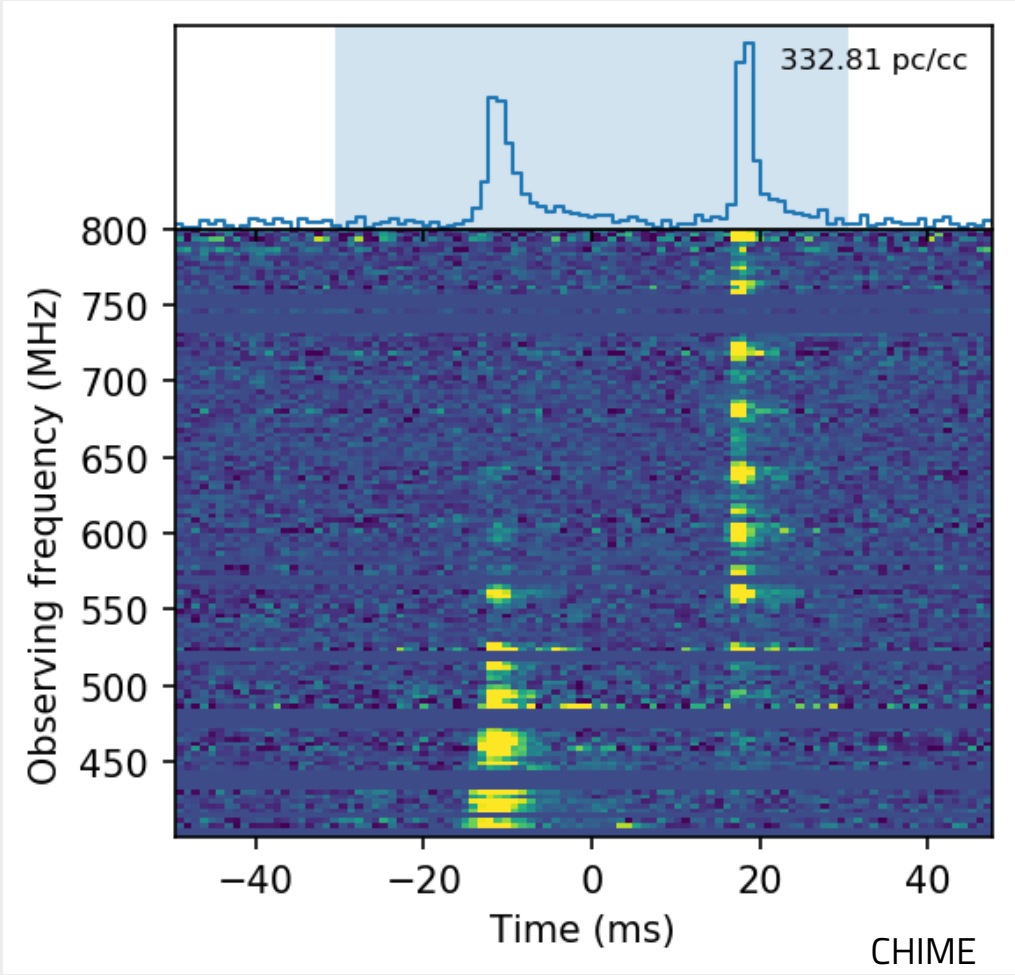

Waterfall plot of the Galactic magnetar SGR 1935+2154 as detected by CHIME/FRB in April 2020. This bright pulse suggests that magnetars could be repeating FRB progenitors.

Mereghetti S, Savchenko V, Ferrigno C, et al. INTEGRAL Discovery of a Burst with Associated Radio Emission from the Magnetar SGR 1935+2154. *The Astrophysical Journal Letters*. 2020/07/27 2020;898(2):L29. doi:10.3847/2041-8213/aba2cf

Localization – VLBI & "Outrigger" Program

- Very-long baseline interferometry (VLBI).
  - The angular resolution depends on antenna diameter and the wavelength of the signal it is receiving.
  - The larger the telescope and the shorter the wavelength, the better the angular resolution.
  - Linking antennas creates a diameter equal to the largest separation (baseline) between antennas. Signals recorded are processed a correlation facility.

- A CHIME/FRB Outrigger – KKO Station (66 km west of CHIME)
  - Localization to tens of milliarcseconds

Jansky Very Large Array (VLA)

European Space Agency.

Lanman AE, Shion A, Lazda M, et al. CHIME/FRB Outriggers: KKO Station System and Commissioning Results. *arXivorg*. 2024;doi:10.48550/arxiv.2402.07898

Localization

- Locations of FRBs relative to their host galaxies. a–f, Optical images of the host galaxies of six FRBs localized by ASKAP (HG, host galaxy).
- White ellipses denote the 90% confidence region of each burst position, including statistical uncertainty and phase referencing errors, while the red crosses mark the measured centroids of each host galaxy.
- a–d, Deep VLT g-band images; e, f, deep GMOS i band images.

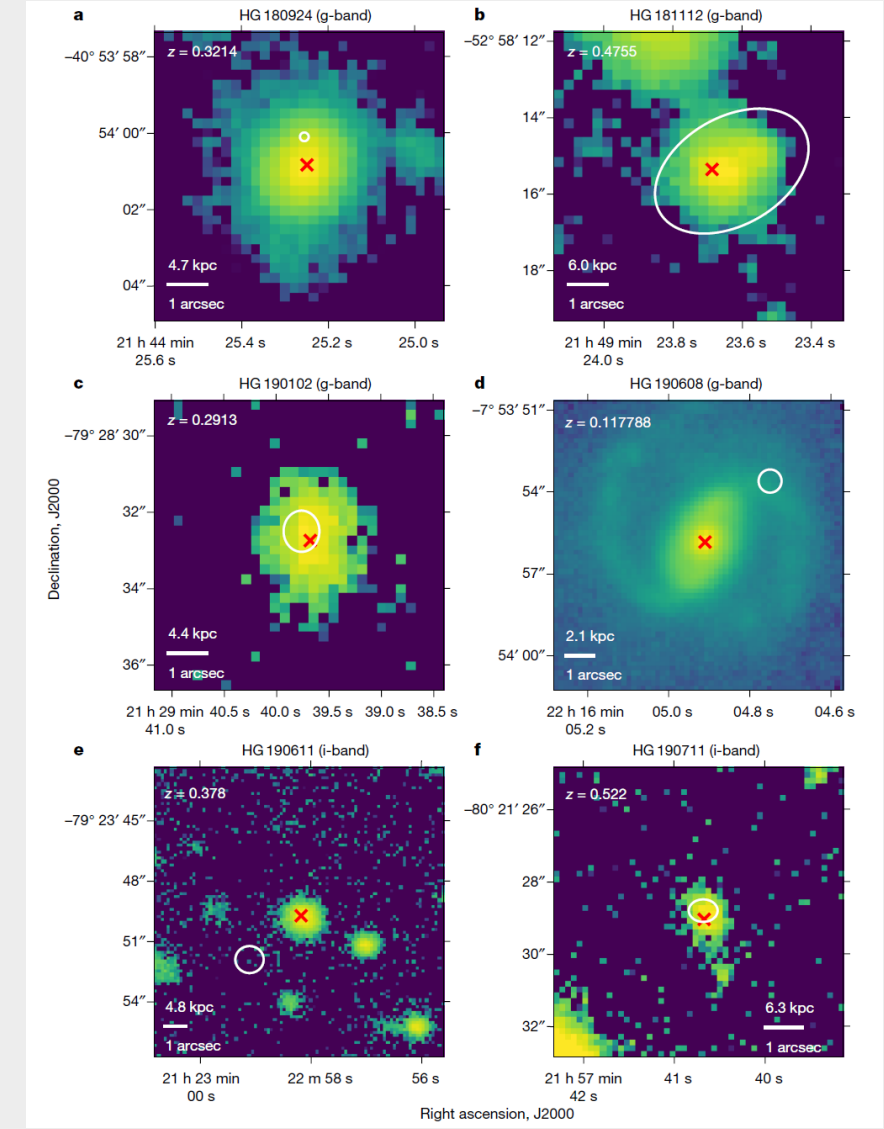

Macquart JP, Prochaska JX, McQuinn M, et al. A census of baryons in the Universe from localized fast radio bursts. *Nature*. 2020/05/01 2020;581(7809):391-395. doi:10.1038/s41586-020-2300-2. Page 393.

First Galactic FRB – SGR 1935+2154, FRB 200428

Swift Alert Telescope - Soft Gamma Repeater, 4/27/2020 (discovered 2014)
CHIME, 2 Bursts from 400-800 MHz, 4/28/2020, and simultaneously
INTEGRAL& Others, X-Ray Burst, STARE2, 1.4 GHz Burst, FRB 200428

https://www.youtube.com/watch?v=CiGj-gtygDU
P. Shaw/UBC/CHIME Collaboration,
Axel Mellinger (Central Michigan University) and NASA

Review of Astrophysical Radiation Mechanisms

TABLE II Astrophysical radiation mechanisms

Mechanisms	Particles	Photons	Examples
blackbody	thermal equilibrium	thermal equilibrium	CMB, stars
thermal	thermal equilibrium	may/may not be in thermal equilibrium	disks, intracluster medium
incoherent non-thermal	non-thermal	subject to self-absorption limit	SNRs, GRBs, blazars
coherent non-thermal	non-thermal	not subject to self-absorption limit	radio pulsars, FRBs

Zhang B. The physics of fast radio bursts. *Reviews of Modern Physics*. July 01, 2023 2023;95:035005. doi:10.1103/RevModPhys.95.035005. Page 29.

Coherent Radiation

- Coherent refers to consistant phase relationship, and *polarization* refers to the orientation of the oscillations.
- Coherent radiation mechanisms involve large numbers (N) of particles emitting with a distinct phase relationship, yielding collective power $\propto N^2$ rather than $\propto N$ for incoherent radiation.
- An extremely coherent radiation mechanism is required to explain the temperature (~10^{34} K). Models include pulsar-like and gamma ray burst-like mechanisms.

Cordes JM, Chatterjee S. Fast Radio Bursts: An Extragalactic Enigma. *ARA & A*. 2019;57(1):417-465. doi:10.1146/annurev-astro-091918-104501, Page 431.

- Coherent emission can be created by particle beams injected into shocked gas.
- Many nanosecond, coherent and polarized signals (shot pulses) are combined incoherently, with variations in shot rate or amplitude, to create millisecond signals or bursts. The short duration pulses are inversely related to the spectral width (~ 1 GHz).
- It is unknown if relativistic beaming plays a role in burst duration and morphology.

Cordes JM, Chatterjee S. Fast Radio Bursts: An Extragalactic Enigma. *ARA & A*. 2019;57(1):417-465. doi:10.1146/annurev-astro-091918-104501

- The underlying particle acceleration may be linear (e.g., field-aligned electrostatic waves) or transverse (curvature and gyro-synchrotron radiation), but a coherence mechanism must also operate.
- An antenna mechanism involves particle bunches ~λ in size (modulo beaming) with many charged particles.
- Maser mechanisms require special distributions in momentum space to provide amplification. A has the advantage of cumulative growth of radiation amplitudes over a region >>λ, which may alleviate energy requirements that challenge coherent curvature radiation from bunches.

Cordes JM, Chatterjee S. Fast Radio Bursts: An Extragalactic Enigma. *ARA & A*. 2019;57(1):417-465. doi:10.1146/annurev-astro-091918-104501.

Coherent Circular Polarization

- *Coherent curvature emission* by *bunches* (charged particles emitted in the same phase) – possibly powered by starquakes has been proposed for repeating FRB and an explanation for narrowband radiation with time frequency drifting.
- This highly *circular polarization (CP)* could be explained by the coherent summation of outcome waves, generated or scattered by *bunches*, having different phases of and electric vectors. (Qiao & Lin)
- Cyclotron resonance can result in the absorption of R-mode photons at a low altitude region of the magnetosphere, and an FRB should then be emitted from a high-altitude region if the waves have strong linear polarization.
- CP could be produced from Faraday conversion (*Faraday Rotation Measurements- RM*).

Wang W-Y, Jiang J-C, Lu J, et al. Repeating fast radio bursts: Coherent circular polarization by bunches. *Science China Physics, mechanics & astronomy*. 2022;65(8):289511. doi:10.1007/s11433-021-1912-0

Possible Origins of Coherent Emission

- Magnetosphere of the neutron star
  - Frequency down drifting occurs because emission with different frequencies originate from different altitudes and the high-frequency emission is observed earlier than low-frequency ones'. [1]
- Synchrotron maser in relativistic shock.
  - Drift is interpreted as due to emitting frequency decreasing with radius in relativistic shocks.
  - Free–free absorption in relativistic shocks introduces a down-drifting. If so, there should be a hot relativistic shell through which the radio waves pass through; and the energy of this shock should be >= 10^{44} erg.
  - Properties of the coincident radio and X-ray flares from SGR 1935+2154, including their approximate simultaneity and relative fluence, as well as the duration and spectrum of the X-ray emission, are consistent with extant (existing) predictions. [2]

(1) Kundu E, Zhang B. Free–free absorption in hot relativistic flows: application to fast radio bursts. *Monthly Notices of the Royal Astronomical Society: Letters*. 2021;508(1):L48-L52. doi:10.1093/mnrasl/slab091
(2) Margalit B, Beniamini P, Sridhar N, Metzger BD. Implications of a Fast Radio Burst from a Galactic Magnetar. *The Astrophysical Journal Letters*. 2020/08/19 2020;899(2):L27. doi:10.3847/2041-8213/abac57

Energy Density U and Magnetic Energy B

$$U_{\rm r,s} \sim \frac{S_\nu \Delta\nu}{c}\left(\frac{d_{\rm so}}{r}\right)^2 \approx 3.2\times10^{10}\ {\rm erg\ cm^{-3}}\, S_{\nu,{\rm Jy}}\Delta\nu_{,{\rm GHz}}\left(\frac{d_{\rm so,\,Gpc}}{r_{10}}\right)^2$$

flux density $S_\nu(t)$ in a bandwidth $\Delta\nu$ scaled to a distance $r = 10^{10} r_{10}$ cm from the source (SO).

(Jy or Jansky is a non SI unit of spectral flux density = 10^{-26} $\rm Wm^{-2}Hz^{-1}$)

The equivalent magnetic energy $U_B = B^2/8\pi$ requires a field strength,

$$B \sim \left(\frac{8\pi S_\nu \Delta\nu}{c}\right)^{1/2}\left(\frac{d_{\rm so}}{r}\right) \approx 9\times10^{15}\ {\rm G}\ \left(S_{\nu,{\rm Jy}}\Delta\nu_{,{\rm GHz}}\right)^{1/2}\ d_{\rm so,\,Gpc},$$

that would be encountered for example at a distance r from a magnetar with surface field $B = 10^{15}\ B_{15}$ G and radius $R = 10^6 R_6$ cm,

$$r \approx 3.3\times10^8\ {\rm cm}\ R_6^{3/2}\left(B_{15}/d_{\rm so,Gpc}\right)^{1/2}\left(S_{\nu,{\rm Jy}}\Delta\nu_{,{\rm GHz}}\right)^{-1/4}$$

Cordes JM, Chatterjee S. Fast Radio Bursts: An Extragalactic Enigma. *ARA & A*. 2019;57(1):417-465. doi:10.1146/annurev-astro-091918-104501, Page 430.

Expressed in terms of the velocity of light cylinder radius

$r_{\rm lc} = cP / 2\pi$ of a spinning object with period P,

$$\frac{r}{r_{\rm lc}} = 0.07 P^{-1/2} R_6^{3/2} (B_{15} / d_{\rm SO,Gpc})^{1/2} \left(S_{\nu,\rm Jy} \Delta\nu_{,\rm GHz} \right)^{-1/4}$$

To match or exceed the radiation energy density with a particle energy density $U_{\rm p} = \gamma m_{\rm e} c^2$, electrons would have to be highly relativistic even with a large electron density. For example, a Lorentz factor $\gamma = (1 - \beta^2)^{-1/2} = 10^7$ (with $\beta = v/c$) requires an electron density $n_{\rm e} \approx 4 \times 10^9$ cm^{-3} for the same parameters as in the above equations. The single-particle or particle-bunch radiation is therefore highly beamed into a solid angle $\Omega_{\rm b} \sim \gamma^{-2}$. However, the total solid angle for an FRB is much larger than this because bursts are incoherent sums of many individual coherent units of radiation (Cordes & Wasserman 2016).

Cordes JM, Chatterjee S. Fast Radio Bursts: An Extragalactic Enigma. *ARA & A*. 2019;57(1):417-465. doi:10.1146/annurev-astro-091918-104501, Page 430.

Isotropic emission implies a total emitted energy obtained by integrating over a spherical shell of thickness cW. Correcting for the beaming solid angle gives the burst energy,

$$E_{\rm b} \sim 4\pi S_\nu W \Delta\nu d_{\rm SO}^2 (\Omega_{\rm b} / 4\pi \approx 1.2\times10^{39}\ {\rm erg}\ S_{\nu\,{\rm Jy}} W_{\rm ms} \Delta\nu, {}_{\rm GHz}\, d^2_{\rm SO,\,Gpc} (\Omega_{\rm b} / 4\pi),$$

$\therefore$ Small bean angles can substantially alter burst energies.

Radiation Brightness Temperature T_b

- Useful for distinguishing incoherent and coherent emission.
- It is the effective blackbody temperature based on the Rayleigh–Jeans portion of the Planck spectrum $I_\nu = 2kT_b/\lambda^2$, where k is Boltzmann's constant and $\lambda = c/\nu$ is the wavelength.
- For a transient burst of duration W and peak flux density S_{pk}, the specific intensity is $I_\nu \sim S_{pk}/\Omega$, where Ω is the observed solid angle of the source.
- A burst source of size $\sim cW$ at distance d subtends $\Omega \sim (cW/d)^2$, giving a brightness temperature $T_b \sim S_{pk} d^2/2k(\nu W)^2$.
- A 1-Jy FRB of millisecond duration yields $T_b = 3.4 \times 10^{35}$ K, compared to $T_b = 3.4 \times 10^{23}$ K for a Galactic pulsar at a kiloparsec distance.

Cordes JM, Chatterjee S. Fast Radio Bursts: An Extragalactic Enigma. *ARA & A*. 2019;57(1):417-465. doi:10.1146/annurev-astro-091918-104501, Page 431.

Luminosity as a Function of Burst Time Scale for Short Duration Coherent Radio Emitters

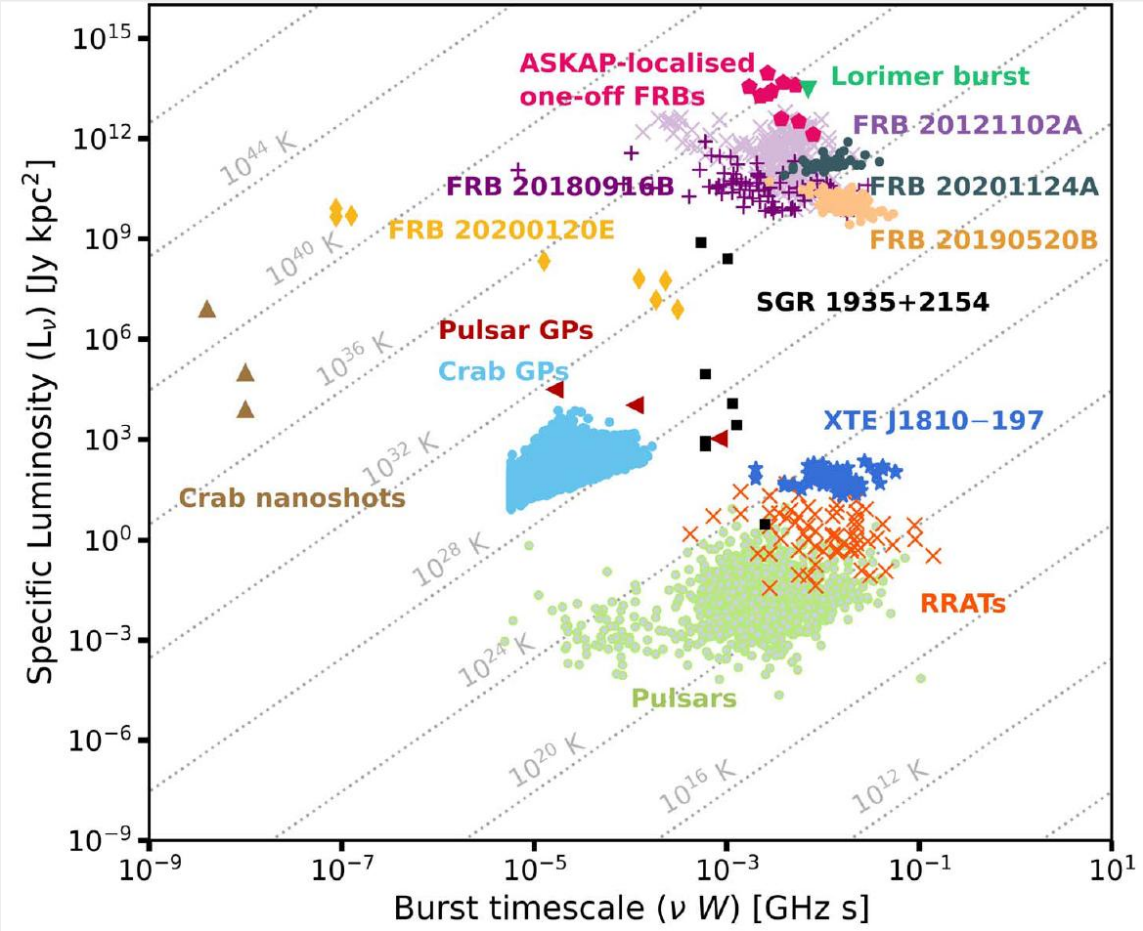

- The Lorimer Burst (green triangle) is a trillion times more energetic than radio pulsars (light green circles) and Rotating Radio Transits (RRATs) (orange crosses) within the Milky Way.
- Repeating (purple, yellow) and non-repeating FRB (magenta). Radio bursts from the galactic magnetars SGR 1935+2154 (black squares) and XTE J1810-197 (blue stars).
- The sloped dotted gray lines indicate the brightness temperature, which is proportional to the specific intensity of a source

Bailes M. The discovery and scientific potential of fast radio bursts. *Science*. 2022;378(6620):eabj3043. doi:doi:10.1126/science. abj3043

Time-luminosity phase space for radio transients: pseudo-luminosity $\ell = S_{pk}D^2$ in Jy kpc^2 vs νW or frequency times pulse width, in GHz-s.

"Coherent" and "incoherent" are separated by the canonical ~10^{12}-K limit for the synchrotron self-Compton process occurring in AGNs. (Max. particles in any given volume.)

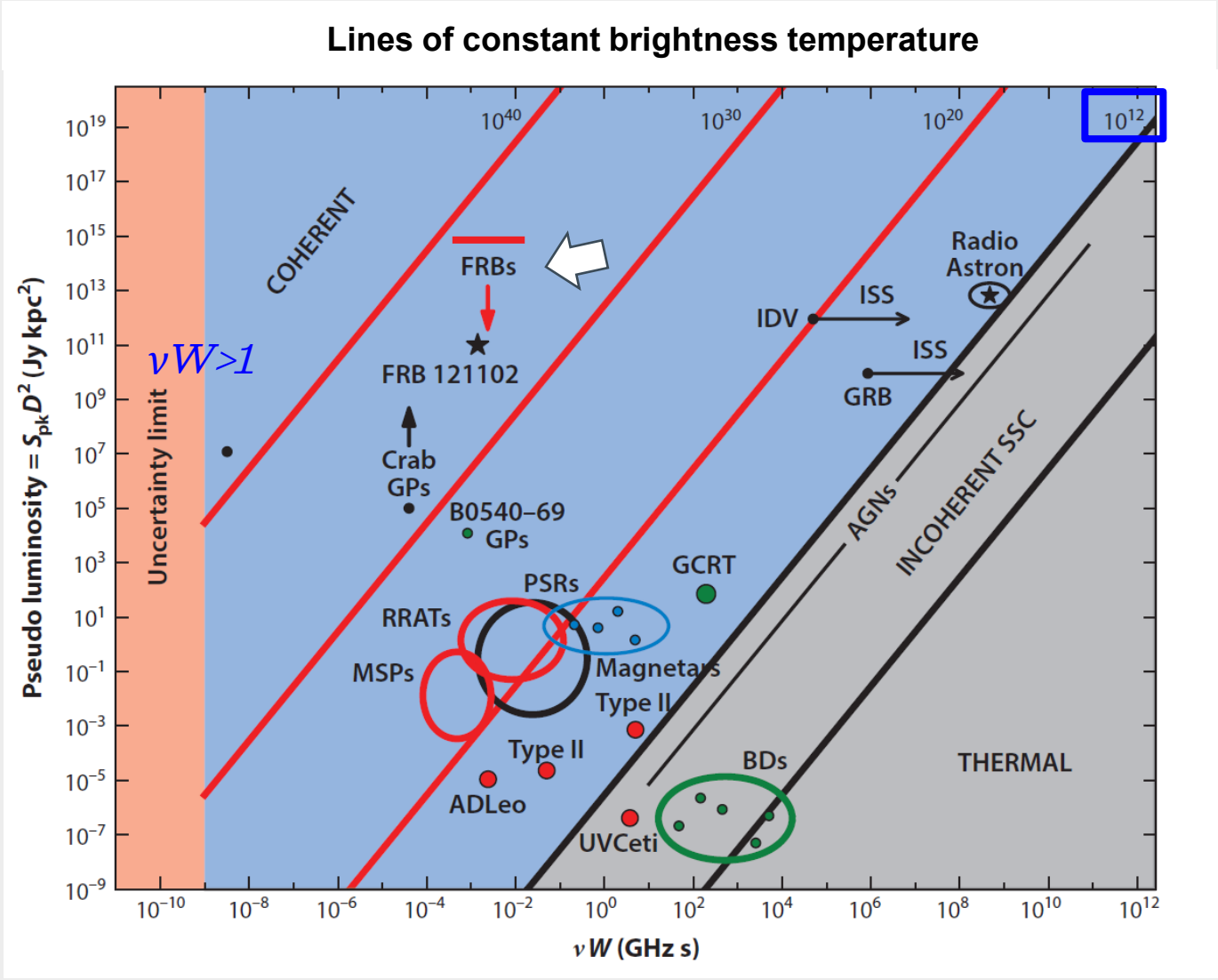

Cordes JM, Chatterjee S. Fast Radio Bursts: An Extragalactic Enigma. *ARA & A*. 2019;57(1):417-465. doi:10.1146/annurev-astro-091918-104501, Page 432.

- ℓ pseudo luminosity in pulsar contexts to emphasize that the measured flux density is influenced by both the angular width of the beam and its direction with respect to the line of sight.
- AGN, active galactic nucleus; BD, brown dwarf; FRB, fast radio burst; GCRT, Galactic center radio transient; GP, giant pulse; GRB, gamma-ray burst; IDV, intraday variable; ISS, interstellar scintillation; MSP, millisecond pulsar; PSR, pulsar radio source; RRAT, rotating radio transient; SSC, synchrotron self-Compton.
- The "uncertainty" limit on the left indicates that $\nu W \geq 1$, as follows from the uncertainty principle.
- Lines of constant brightness temperature $T_b = SD^2/2k(\nu W)^2$ are shown, where k is Boltzmann's constant.
- Points are shown for the nanoshots (Hankins & Eilek 2007) and GPs detected from the Crab pulsar and a few millisecond pulsars, and single pulses from other pulsars.
- Points are shown for solar bursts, radio flares from stars, brown dwarfs, and AGNs.
- Arrows pointing to the right for the GRB and IDV points indicate that ISS implies smaller brightness temperatures than if characteristic variation times are used to estimate the brightness temperature.
- Fast radio transients include RRATs (McLaughlin et al. 2006), the GCRT source J1745-3009 (Hyman et al. 2005), and radio emission from Galactic magnetars (Olausen & Kaspi 2014).

Burst Considerations

- Duration,
- Time-frequency structure,
- Polarization,
- Energetics, and,
- For repeating FRBs, their low duty cycle, absence of periodicity, and rate variability.
- Population properties, including the sky rate versus fluence distribution, which are linked to their spatial distribution and beaming properties.

Cordes JM, Chatterjee S. Fast Radio Bursts: An Extragalactic Enigma. *ARA & A*. 2019;57(1):417-465. doi:10.1146/annurev-astro-091918-104501. Page 453

Beaming

- Relativistic beaming with large Lorentz factors γ is likely necessary given the burst energetics. Unknown is if beaming plays a role in burst durations and morphology.
- The emitted luminosity of an individual source is determined by the radiation physics, but the measured flux density depends on beam orientations.

Cordes JM, Chatterjee S. Fast Radio Bursts: An Extragalactic Enigma. *ARA & A*. 2019;57(1):417-465. doi:10.1146/annurev-astro-091918-104501.

Possible Beaming Geometries

a. Non-rotating jetted beam with magnetic reconnection, or from a jet aligned with the spin axis of a compact object.

b. Rotating pulsar-like beam sweeping through a solid angle greater than the beam itself.

c. Quais-isotropic radiation of local coherent beams, such as from particle beams in shocked gas.

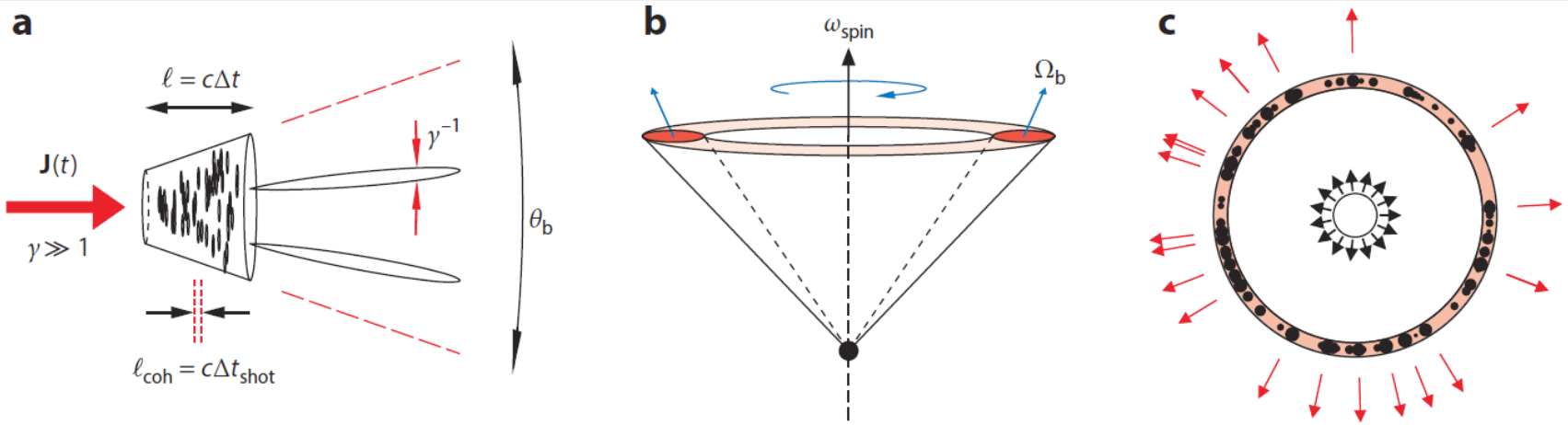

Figure 17

Possible beaming geometries for FRB sources. (*a*) A relativistic jet spanning an angle θ_b much larger than single particle beaming angles $\sim\gamma^{-1}$. Individual coherent emitters of size ℓ_{coh} are contained in an extended region of depth $\ell \sim cW$, where W is the FRB duration. The jet beam solid angle is $\sim\theta_b^2$. (*b*) A rotating beam comprising a relativistic jet swept around by rotation and covering a total solid angle $\Omega \sim 2\pi\sqrt{\Omega_b}$. (*c*) Quasi-isotropic mission from a spherical shell containing individual coherent emitters with a total solid angle $\Omega \sim 4\pi f_{coh}$, where f_{coh} is the fraction of the shell with active emitters. Abbreviation: DM, dispersion measure.

Cordes JM, Chatterjee S. Fast Radio Bursts: An Extragalactic Enigma. *ARA & A*. 2019;57(1):417-465. doi:10.1146/annurev-astro-091918-104501.

FRB Magnetized Neutron Star Source Model

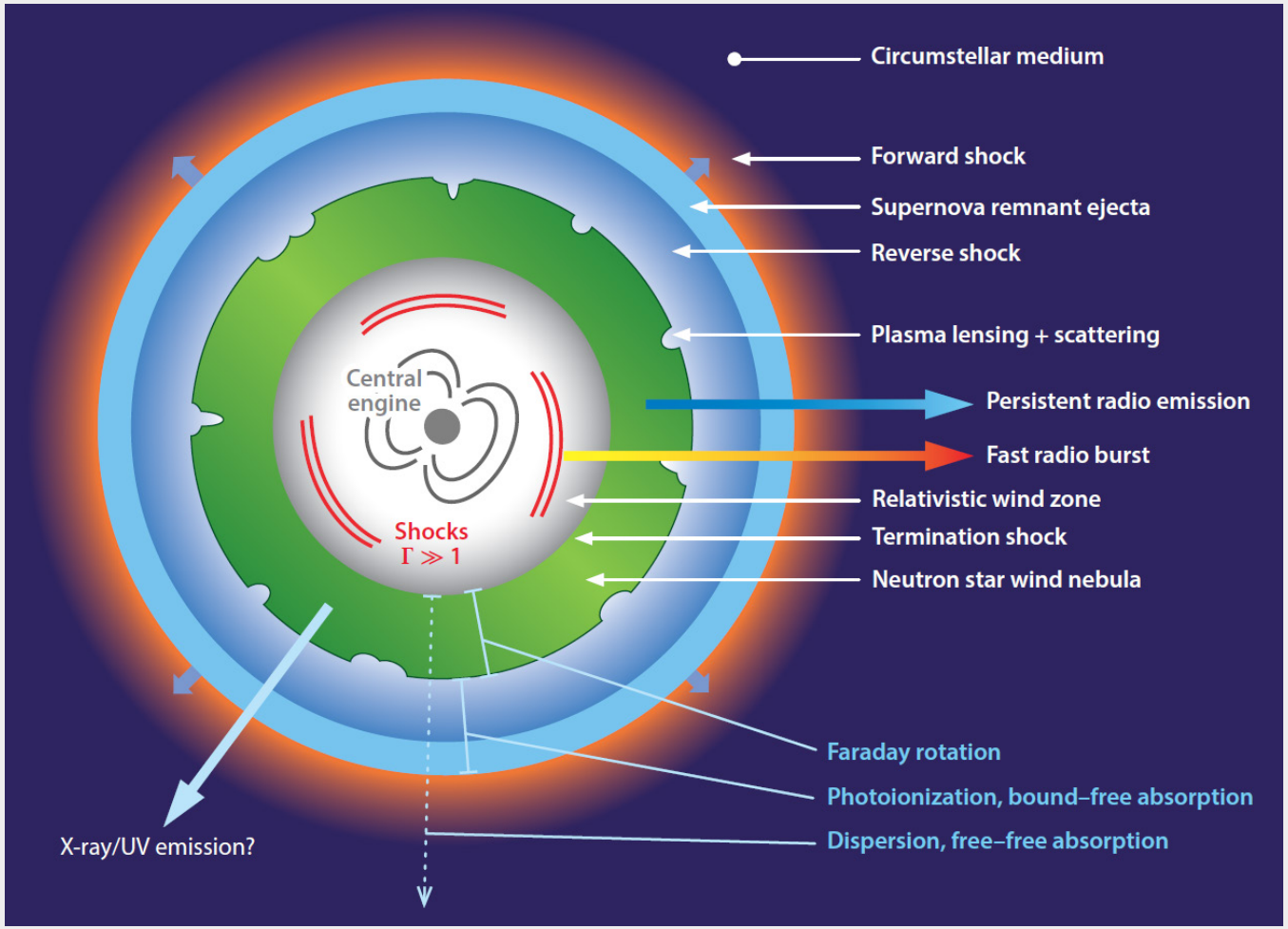

Models include young, rapidly rotating neutron stars (giant pulse model, magnetar models and superluminous supernovae.

Shown is a diagram of an FRB source engine involving a young, highly magnetized neutron star.

Alternative models, such as compact objects orbiting AGNs, may share some (but not all) of the same features.

Figure adapted from Margalit & Metzger (2018) . Cordes JM, Chatterjee S. Fast Radio Bursts: An Extragalactic Enigma. *ARA & A*. 2019;57(1):417-465. doi:10.1146/annurev-astro-091918-104501. Page 458.

Release of Relativistic Particles

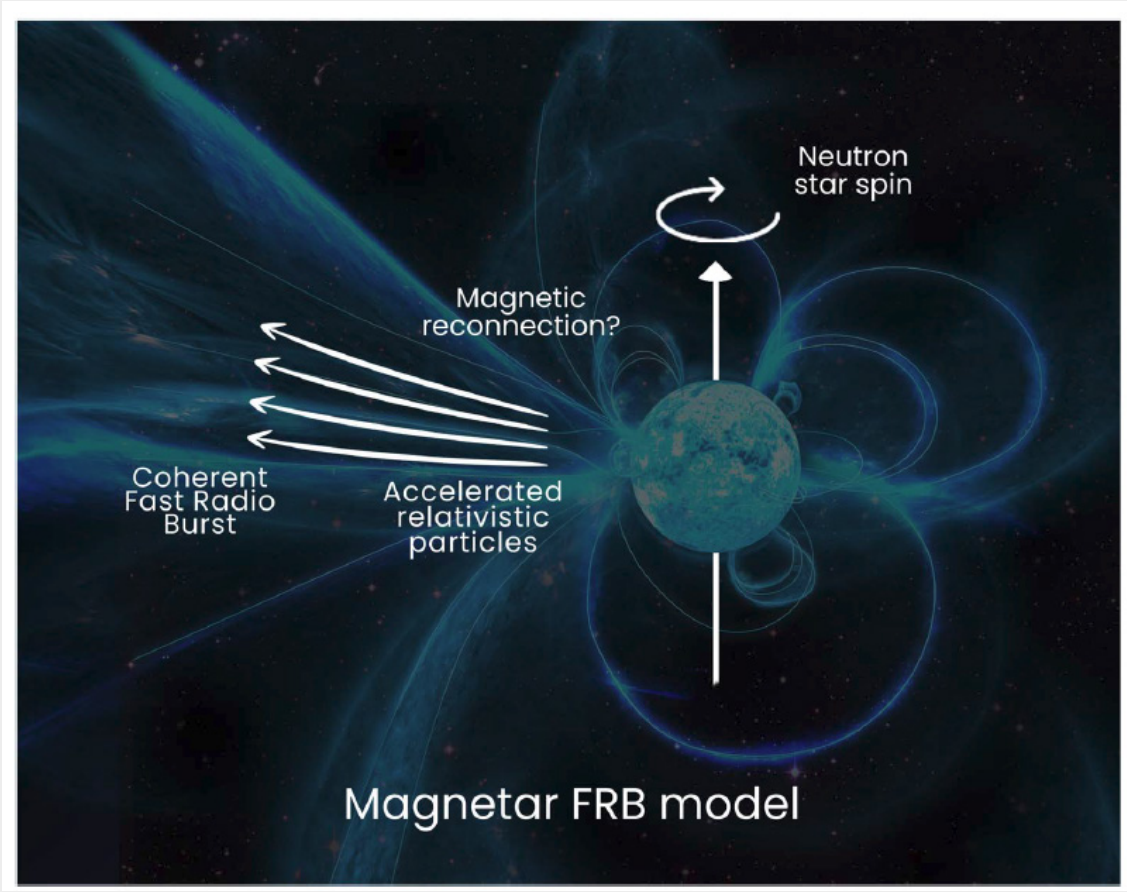

Reconfiguration of the intense magnetic fields around a magnetar is associated with high-energy outbursts. In this model for FRB generation, reconfiguration of the magnetic field releases relativistic particles that generate coherent radio emission in the magnetosphere, possibly producing FRBs.

Bailes M. The discovery and scientific potential of fast radio bursts. *Science*. 2022;378(6620):eabj3043. doi:doi:10.1126/science.abj3043

Repeaters

- It is unknown if all non-repeaters may actually be repeaters.
- CHIME/FRB reported on 25 repeating FRBs in 2023 (2-12 bursts).[1]
- Repeaters have complex time–frequency structure, with sub-bursts that drift downward in frequency as time progresses, seems ubiquitous among bursts from repeating sources. “Sad trombone.” (Not to be confused with dispersion medium findings.)[1]
- On average, repeater bursts are observed to be longer in duration and narrower in bandwidth than for bursts seen from nonrepeating sources.
- Burst widths are statistically larger than non-repeating. [2]

1. The CFRBC, Andersen BC, Bandura K, et al. CHIME/FRB Discovery of 25 Repeating Fast Radio Burst Sources. *The Astrophysical Journal*. 2023/04/26 2023;947(2):83. doi:10.3847/1538-4357/acc6c1.
2. Fonseca E, Andersen BC, Bhardwaj M, et al. Nine New Repeating Fast Radio Burst Sources from CHIME/FRB. *The Astrophysical Journal*. March 01, 2020 2020;891:L6. doi:10.3847/2041-8213/ab7208

Repeating FRB Orbital Model

In this repeating FRB model (99), a massive star's stellar wind (blue arrows) causes an orbiting (with a period of weeks to months) magnetar (small black dots) to emit FRBs. The interaction between the stellar wind and the magnetar wind produces cavities (cyan shading) separated by a shock front (cyan lines). The cavity preferentially emits high-frequency FRBs (blue and green wavy arrows) at the leading edge and lower-frequency FRBs (red wavy arrows) in the trailing sections. This model is an attempt to explain both the activity windows of some repeaters and their radio frequency time dependence.

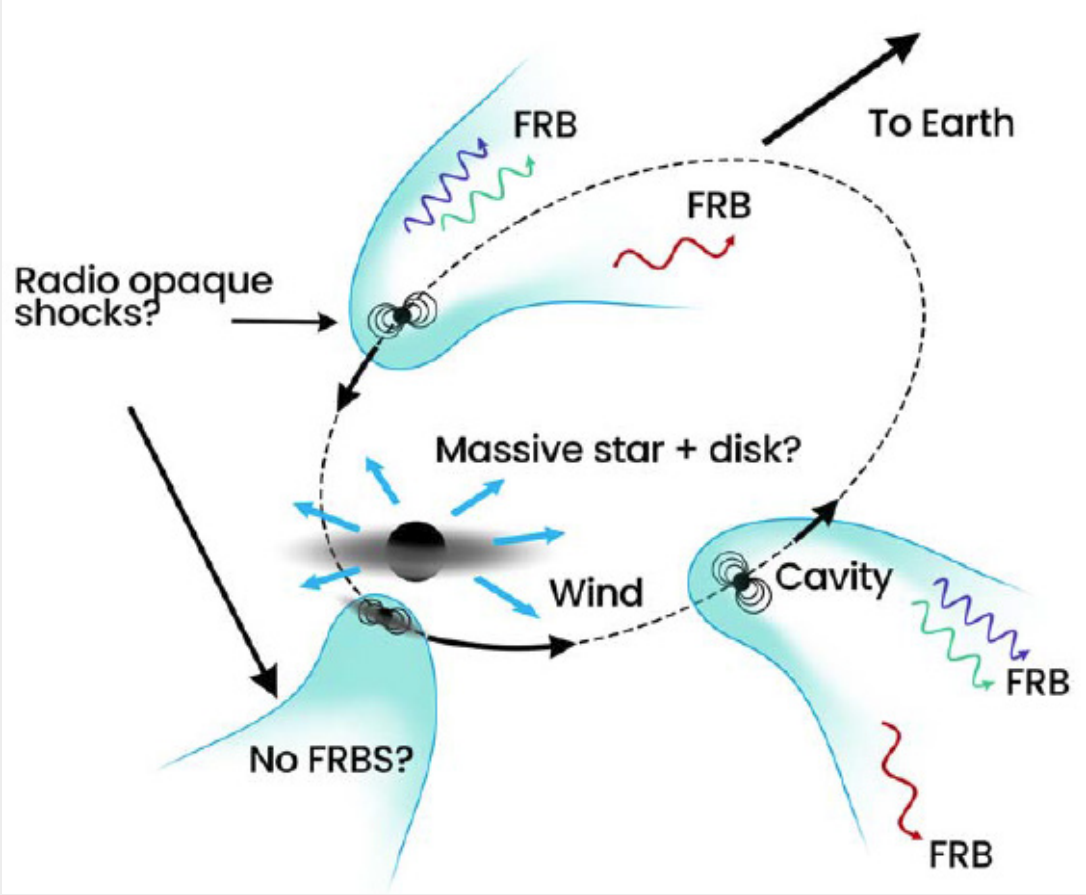

Bailes M. The discovery and scientific potential of fast radio bursts. *Science*. 2022;378(6620):eabj3043. doi:doi:10.1126/science.abj3043

Sub-burst Frequency Drift seen in Repeaters.

A. Sub-burst central frequency as a function of arrival time. similar slopes at the same central observing frequency.
B. Measured linear burst drift rates vs. burst characteristic radio frequency.
C. The FWHM bandwidths measured by fitting a 2D Gaussian model to each sub-burst.
D. 2D Gaussian FWHM temporal durations of each sub-burst .
E. A0-A5 dynamic profile, averaged over frequency.

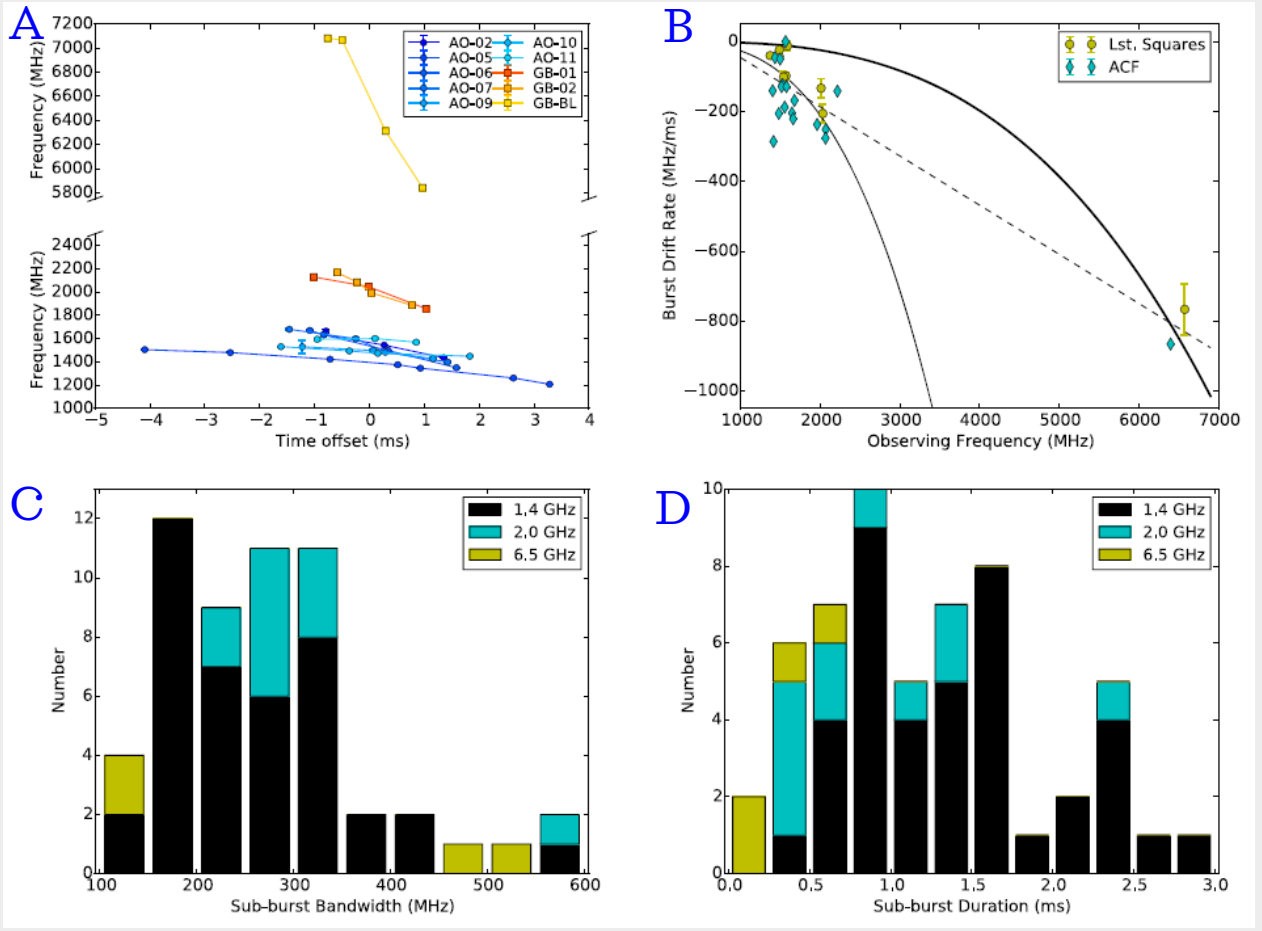

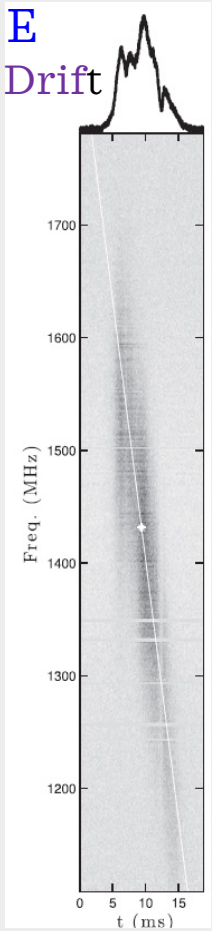

Hessels JWT, Spitler LG, Seymour AD, et al. FRB 121102 Bursts Show Complex Time-Frequency Structure. *The Astrophysical Journal*. May 01, 2019 2019;876:L23. doi:10.3847/2041-8213/ab13ae

Discussion

Sons David & Paul at *Green Bank, WV*

FAST
China

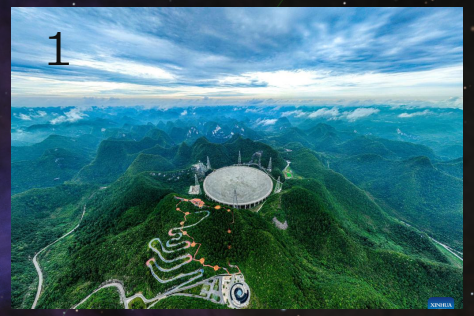

ASKAP
Australia

WRST/APERTIF
Netherlands

UTMOST
New South Whales

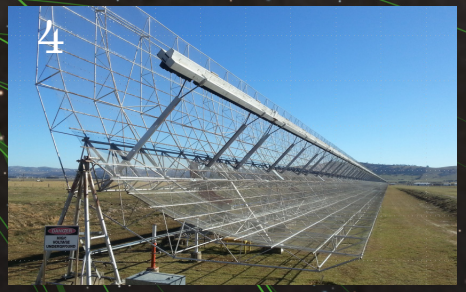

NASA/JPL-Caltech Magnetar Depiction

(1) XINHUA; (2) CSIRO; (3) van Cappellen; (4) Molonglo Observatory

Supplemental Material

- More on Localization
  - LOFAR
  - Dark Energy Spectroscopic Instrument (DESI)
  - DESI r-Band Localization of 3 FRB
- Statistical Approach to Sources
  - Energy and Redshift Distributions
  - Energy Distribution Calculation

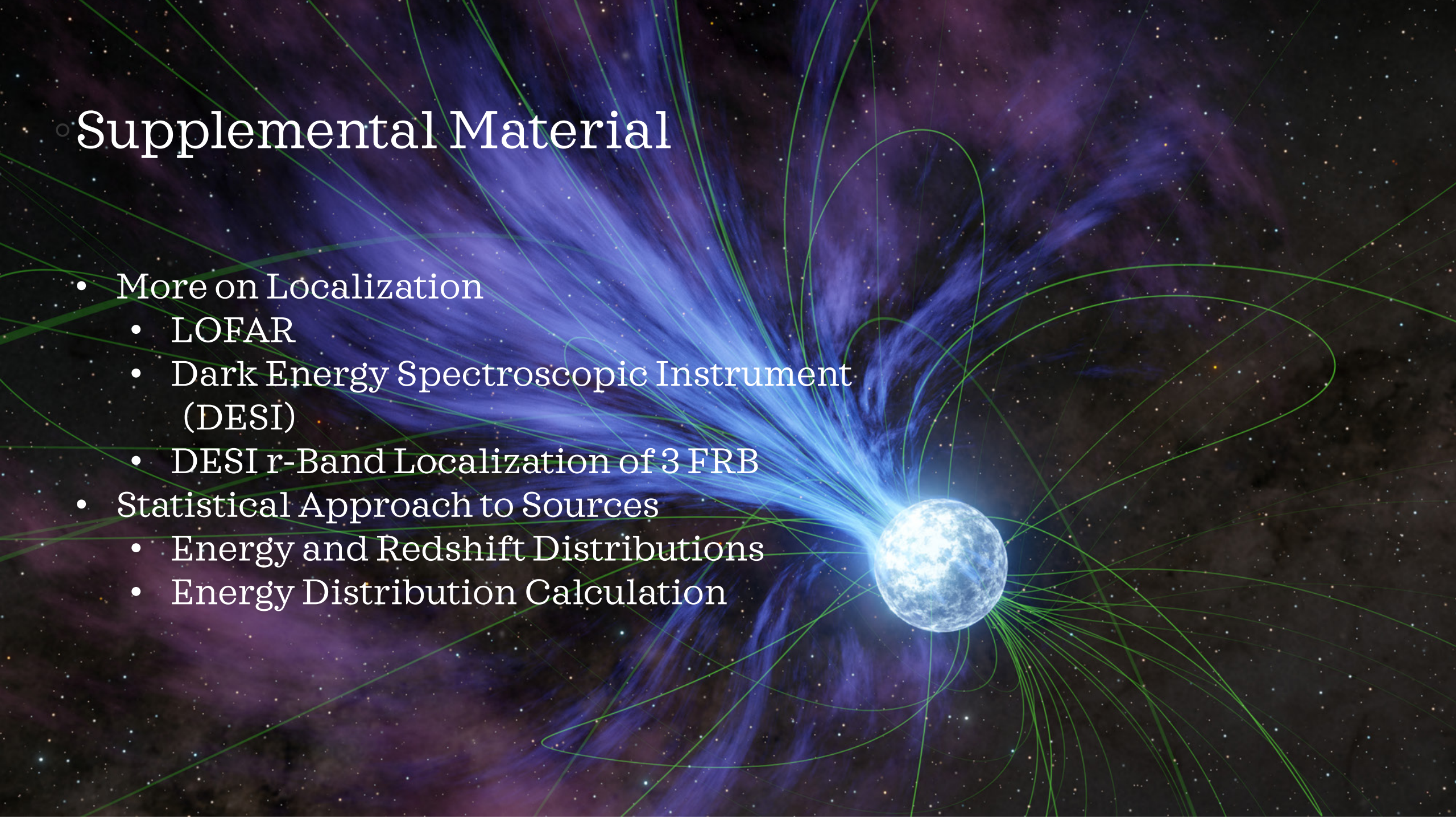

Low Frequency Array (LOFAR)

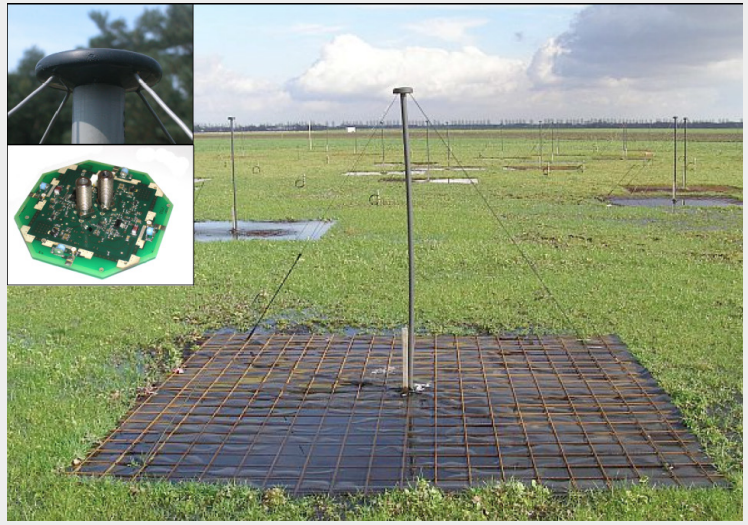

Beam sizes are represented by gray area.

European radio telescope in the Netherlands, operating in the frequency range between 10 and 240 MHz. Several thousand dipole antenna arranged in tiles, and configured as three types of “stations” (core, remote international), based on different interferometer baselines, number of tiles and beamforming ability.

van Haarlem, MP LOFAR - The LOw-Frequency ARray ,2013
B. W. Stappers et al.: Observing pulsars and fast transients with LOFAR, Astronomy & Astrophysics, 2018

Dark Energy Spectroscopic Instrument (DESI)

- Measures the expansion history of the universe using the baryon acoustic oscillations (BAO) imprinted in the clustering of galaxies, quasars, and the intergalactic medium.
- One of the key methods for studying dark energy
- On June 13, 2023 EDR (Early Data Release) – spectra of 2 million galaxies, quasars and stars. Mass migration of stars into Andromeda galaxy observed.
- The focal plane accommodates 5,000 small computer controlled fiber positioners.
- The DESI instrument is capable of taking 5,000 simultaneous spectra over a wavelength range from 360 nm to 980 nm.

DESI in the dome of the Nicholas U. Mayall 4-meter Telescope at the Kitt Peak National Observatory – Arizona.

Lawrence Berkeley National Lab/KPNO/NOIRLab/NSF/AURA

DESI r-Band Localization of 3 FRB

(Dark Energy Spectroscopic Instrument on Kitt Peak Arizona)

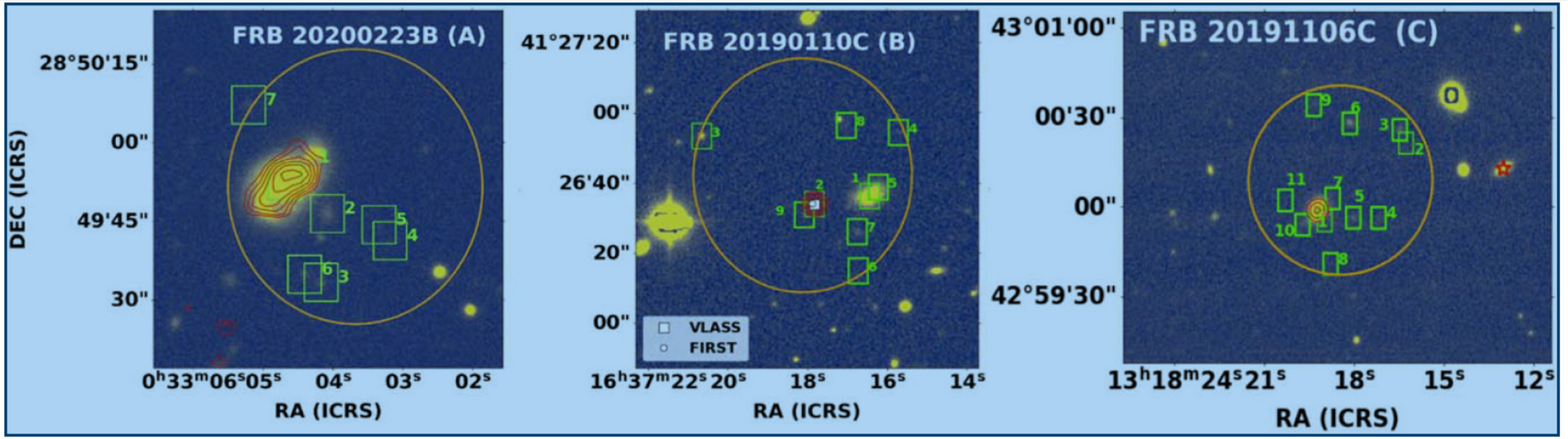

Green boxes show the positions of host galaxy candidates – #1's most probable. The red background contours are from high-resolution LOFAR Two-meter Sky Survey. There are multiple sources in each survey, and a probable host galaxy is seen in each.

Ibik AL, Drout MR, Gaensler BM, et al. Proposed Host Galaxies of Repeating Fast Radio Burst Sources Detected by CHIME/FRB. *The Astrophysical Journal*. 2024/01/17 2024;961(1):99. doi:10.3847/1538-4357/ad0893

DESI EDR example galaxy LEDA 1787534

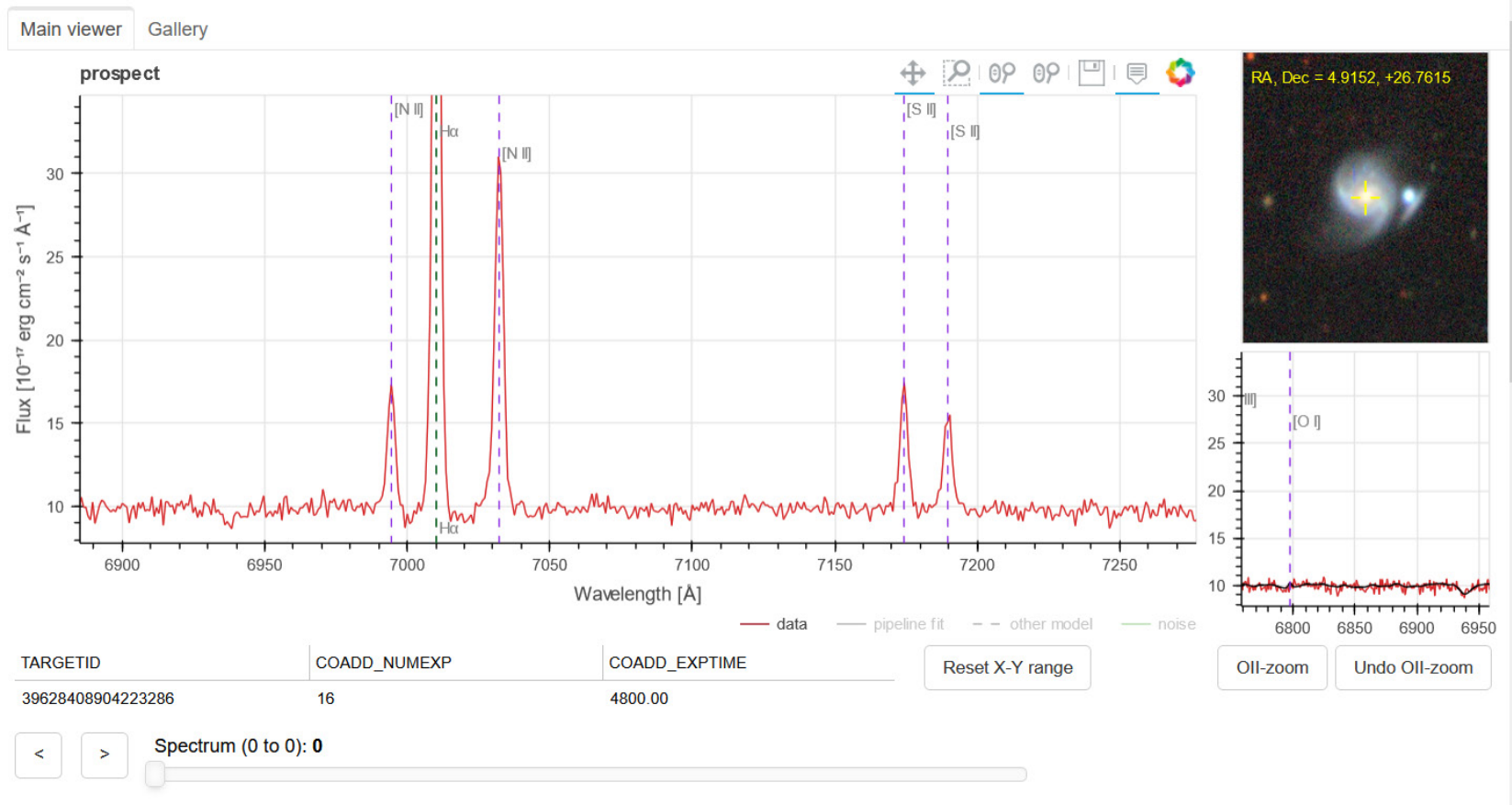

DESI (Dark Energy Spectroscopic Instrument) spectrum example showing H-alpha, [N II] and [S II] emission coming from the galaxy LEDA 1787534, showing that it is an emission-line galaxy. H-alpha is truncated for display purposes.

https://www.legacysurvey.org/viewer/desi-spectrum/edr/targetid39628408904223286

Statistical Approach to Sources - Energy & Redshift Distributions

- Two key intrinsic distributions of FRB sources shape the observed FRB population.
  - The first is the isotropic-equivalent energy (or luminosity)of the bursts.
  - The second is the intrinsic redshift distribution of FRB sources, which is closely related to the largely unknown astrophysical sources that produce cosmological FRBs.
- The leading model for the repeaters involve magnetars, neutron stars with super strong magnetic fields. (e.g. Galactic FRB 20200428 in association with hard X-bursts).
- Since most magnetars are believed produced from SN, this model predicts the FRB rate follows the cosmic star formation rate (SFR).
  - Mergers of binary neutron stars can form rapidly spinning magnetars.

Zhang RC, Zhang B, Li Y, Lorimer DR. On the energy and redshift distributions of fast radio bursts. *Monthly Notices of the Royal Astronomical Society*. 2021;501(1):157-167. doi:10.1093/mnras/staa3537

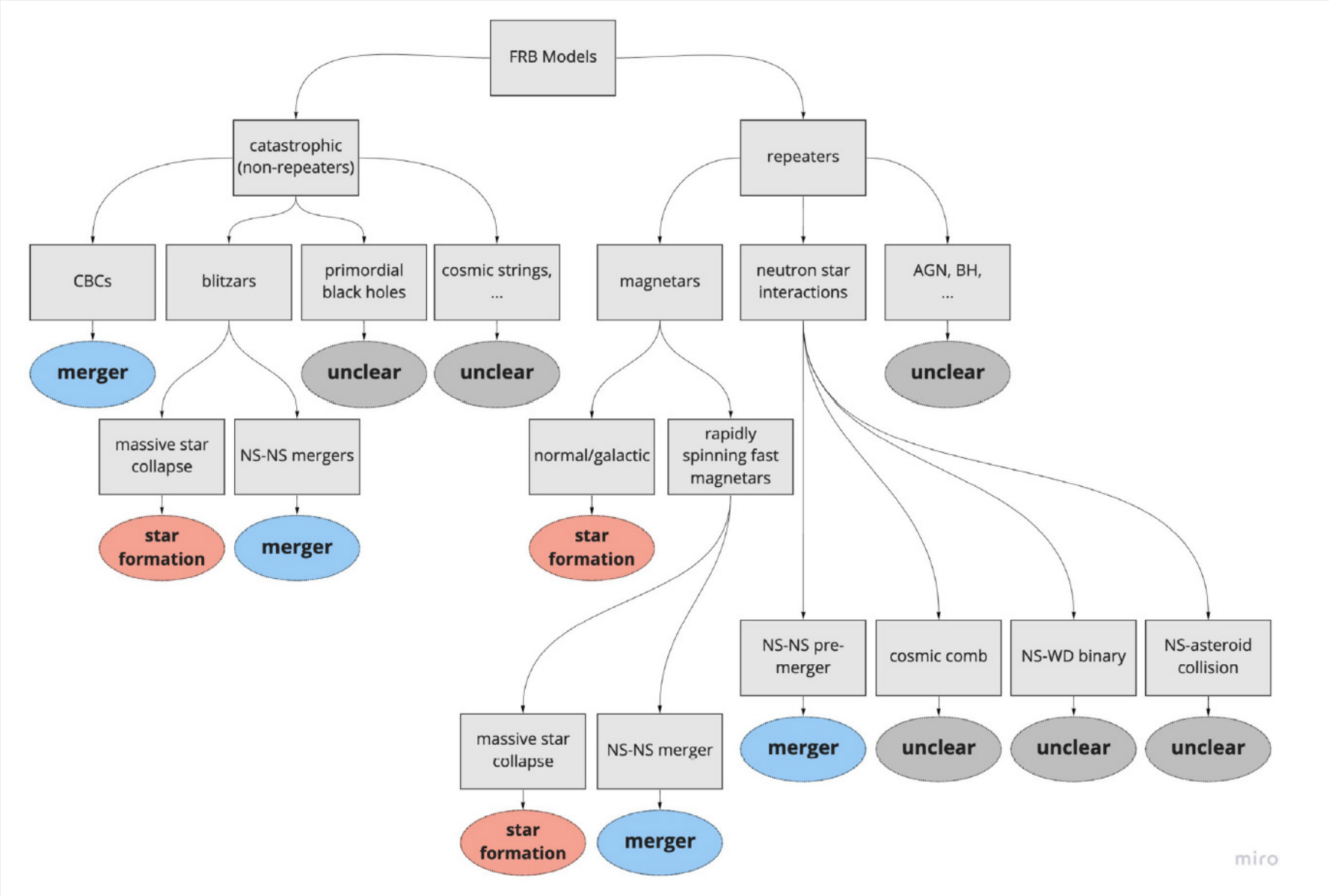

A flow chart for the various redshift distributions implied by different FRB models. Zhang et al.

Energy Distribution

- Luminosity function of FRBs is an event rate per unit cosmic co-moving volume per unit luminosity. Since observed durations of FRBs are typically milliseconds, this luminosity function may be translated to an isotropic energy distribution in the form of

$$\frac{\mathrm{d}N}{\mathrm{d}E} \propto \left(\frac{E}{E_{\mathrm{C}}}\right)^{-\alpha} e^{-\frac{E}{E_{\mathrm{c}}}}$$

where E_{C} is the exponential cut-off energy. $\alpha \sim 1.8$. Luminosity cut-off at $L_C \sim 3 \times 10^{44}$ erg s^{-1}, corresponds to $E_{\mathrm{C}} \sim 3 \times 10^{41} erg$.

Zhang RC, Zhang B, Li Y, Lorimer DR. On the energy and redshift distributions of fast radio bursts. *Monthly Notices of the Royal Astronomical Society*. 2021;501(1):157-167. doi:10.1093/mnras/staa3537